

Copyright
by
Nebiyu Barsula Sermollo
2015

**The Thesis Committee for Nebiyu Barsula Sermollo
Certifies that this is the approved version of the following thesis:**

A Theoretical Formulation for Flexoelectric Membranes

**APPROVED BY
SUPERVISING COMMITTEE:**

Supervisor:

Rui Huang

Chad Landis

A Theoretical Formulation for Flexoelectric Membranes

by

Nebiyu Barsula Sermollo, B.S.E

Thesis

Presented to the Faculty of the Graduate School of

The University of Texas at Austin

in Partial Fulfillment

of the Requirements

for the Degree of

Master of Science in Engineering

The University of Texas at Austin

May 2015

Dedication

To my family and friends for their unending love and support.

Acknowledgements

First and foremost, I would like to thank my advisor, Dr. Rui Huang, for his guidance, wisdom and patience during my time at UT. Dr. Huang has not only guided my research, but he has also given me the care and support that has enabled me to complete this degree. I would like to thank Dr. Chad Landis for being a part of this thesis committee. I am also thankful to the faculty members of the Engineering Mechanics department, in particular, Dr. Gregory Rodin, Dr. K. Ravi-Chandar and Dr. Mark Mear for their kindness and generosity. My gratitude also goes to the entire staff of the Engineering Mechanics department, with special thanks to Scott Messec, Adele Magnani, and Tina Woods for their support.

My time at UT would not have been as bright and rewarding had it not been for the amazing group of friends that I was fortunate enough to find. This includes Stephen, Steve, Vi, Sasha, Alex, Anand, Sundeep, Vishal, Sharavan, Chenglin, Martin, Gary, Charles, Prem, Vivek, Ashish, Wei, Nickolas, Saumik, and many more. Countless afternoons spent discussing solid mechanics, astrophysics, finite element methods, politics, ethics, morals, religion, education, culture, the meaning of life, and many other topics has allowed me to not only learn so much about those topics, but has ultimately forced me to learn about myself. For that, I am truly grateful.

Of course, I would not be where I am today without the unconditional love and support of my family. I am incredibly fortunate and thankful to have the family that I do.

Finally, my gratitude goes to everyone who has helped me on my way in life so far, and especially to the people who had faith in me without any real evidence that it was justified. Thank you.

Abstract

A Theoretical Formulation for Flexoelectric Membranes

Nebiyu Barsula Sermollo, M.S.E

The University of Texas at Austin, 2015

Supervisor: Rui Huang

Flexoelectricity is electric polarization induced by a strain gradient. This phenomenon has been observed in different types of materials. It has been studied and documented that biological membranes possess this flexoelectric property. Research by Brownell et al. has shown that the inner-ear hair cells elongate or shrink as a result of external stimuli. This shrinking and elongation of the cells is due to the wrinkling and flattening of the cell membrane surrounding the hair cells. To study this biomechanical response, a soft, elastomeric membrane under loading by in-plane forces, moments and voltage across the membrane is considered. This membrane is assumed to have the flexoelectric property. Using a thermodynamic approach, a set of constitutive equations are derived that relate the physical quantities (forces, moments, voltage) to the state variables (strains, curvatures, electric displacement). The accuracy of these equations is tested by using them to estimate the flexoelectric coefficient of certain materials following a procedure established by Cross et al. Additionally, a critical membrane thickness is found which ensures a positive-definite Helmholtz free energy for the

membrane, guaranteeing a stable system. Finally, a model for the wrinkling and flattening of the cell membrane surrounding the inner-ear outer hair cells is developed using the derived constitutive equations.

Table of Contents

List of Tables	ix
List of Figures	x
Chapter 1: Introduction	1
1.1 Flexoelectricity in hard materials.....	1
1.2 Flexoelectricity in soft materials.....	3
1.3 A model for outer hair cell membrane	6
Chapter 2: Formulation and Methodology.....	10
2.1 Thermodynamic formulation	10
2.2 A free energy function	14
2.3 Small-strain formulation	19
2.4 Limitations of the free energy function	21
2.5 A sandwich model.....	24
Chapter 3: Results and Discussions	27
3.1 Flexoelectric coefficient measurements.....	27
3.2 Converse flexoelectric effect	40
3.3 Bending of membranes	42
3.4 A membrane-spring model	52
Chapter 4: Conclusions.....	59
References.....	61
Vita	63

List of Tables

Table 1: Values of critical thickness, L_c , for common soft and hard materials23

Table 2: Comparison of displacement values obtained using equation (3.16)

(Baskaran et al.) and equation (3.4) (Cross et al.)40

List of Figures

<u>Figure 1</u> : Schematic of a membrane of thickness t undergoing bending [1].....	2
<u>Figure 2</u> : Misalignment of ions during bending [1].....	2
<u>Figure 3</u> : Calamitic phase - Pear/Rod-like LC molecules in normal (left) and splay deformation (right). Net polarization towards the right [1]	4
<u>Figure 4</u> : Bent-core phase - Banana-shaped LC molecules in normal (left) and splay deformation (right). Net polarization towards the bottom [1]	4
<u>Figure 5</u> : Bilayer lipid cell membrane [1].....	6
<u>Figure 6</u> : Inner ear hair cell. Figure on the right shows the cell membrane [24].....	7
<u>Figure 7</u> : Inner ear cell membrane [6]	8
<u>Figure 8</u> : Schematic of dielectric membrane	10
<u>Figure 9</u> : Schematic of membrane under simple bending with $\kappa_1 > 0$	14
<u>Figure 10</u> : Schematic illustrating the sign convention for polarization and curvature	15
<u>Figure 11</u> : Schematic of the sandwich model	24
<u>Figure 12</u> : Normalized effective flexural rigidity verses normalized membrane thickness.....	26
<u>Figure 13</u> : Experimental setup by Cross et al. for measurement of flexoelectric coefficient [10].....	28
<u>Figure 14</u> : Cross et al. [10] result showing Polarization verses strain gradient for two locations on the beam.....	30
<u>Figure 15</u> : Schematic of the setup used to recreate the Cross et al. experiment....	31
<u>Figure 16</u> : Plot recreating Polarization vs. Strain Gradient data from figure 15 ...	35

<u>Figure 17</u> : Plot of Polarization vs. Strain Gradient determined using equations (3.11) and (3.12).....	35
<u>Figure 18</u> : Schematic of experimental setup by Baskaran et al. in [11]	36
<u>Figure 19</u> : Polarization verses strain gradient from Baskaran et al. [11]. The blue line and points represent values obtained using Cross et al. equation (3.4) while the red line and points represent values obtained using equation (3.16).....	38
<u>Figure 20</u> : Plot recreating Polarization vs. Strain Gradient data from figure 20 ...	39
<u>Figure 21</u> : Polarization vs. Strain Gradient from [11] using equation (3.12).....	39
<u>Figure 22</u> : Schematic of membrane under in-plane loading.....	42
<u>Figure 23</u> : Normalized membrane displacement verses normalized position for increasing values of normalized applied voltage with no in-plane loading, $p = 0$	47
<u>Figure 24</u> : Normalized membrane displacement verses normalized position for increasingly compressive values of in-plane loading with $\Phi = 0.1.50$	
<u>Figure 25</u> : Normalized maximum membrane displacement verses normalized in-plane loading for increasing values of normalized applied voltage	51
<u>Figure 26</u> : Illustration of a part of the cell (plasma) membrane of an outer hair cell [6]. The spectrin molecules are assumed to be connected to the plasma membrane by stiff pillars	52
<u>Figure 27</u> : Schematic of a membrane-spring model, similar to Brownell et al.	53

Chapter 1: Introduction

Flexoelectricity is electrical polarization induced by a strain gradient. It is a size-dependent effect which is more significant in nanoscale systems [1]. In solid ionic crystals, flexoelectricity is caused by non-uniform displacement of ions under a strain gradient. This disrupts inversion symmetry and forms a net polarization. In soft materials, flexoelectricity is caused by the reorientation of irregularly shaped, polarized molecules under strain gradients. These strain gradients come about when these molecules are under splay (bent) deformation. Flexoelectricity is more apparent in materials which have centrosymmetry since these materials are not piezoelectric [1]. Additionally, it is more evident in materials which possess unique geometries where large strain gradients are achievable.

1.1 FLEXOELECTRICITY IN HARD MATERIALS

The effect of flexoelectricity is captured in the total induced electric polarization. In general, the total induced electric polarization is given by

$$P_i = \epsilon_0 \chi_{ij} E_j + d_{ijk} \sigma_{jk} + \mu_{ijkl} \frac{\partial \epsilon_{jk}}{\partial x_l} \quad (1.1)$$

The first term represents the dielectric effect, where ϵ_0 is the permittivity of free space, χ_{ij} is the electric susceptibility, and E_j is the electric field. The second term represents the piezoelectric effect, where d_{ijk} is the piezoelectric coefficient and σ_{ij} is the stress. The final term represents the flexoelectric effect, where μ_{ijkl} represents the flexoelectric coefficient and $\frac{\partial \epsilon_{jk}}{\partial x_l}$ is the strain gradient. While the piezoelectric effect can only be observed in the 20 non-centrosymmetric crystal point groups, the flexoelectric effect exists in all 32 point groups [2]. In centrosymmetric materials for which piezoelectric effects are absent, the induced electric polarization simplifies to

$$P_i = \epsilon_0 \chi_{ij} E_j + \mu_{ijkl} \frac{\partial \epsilon_{jk}}{\partial x_l} \quad (1.2)$$

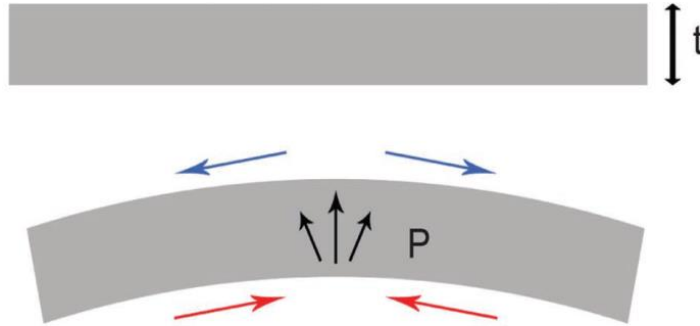


Figure 1: Schematic of a membrane of thickness t undergoing bending [1]

Figure 1 shows a membrane of thickness, t . When this membrane is bent, a non-zero strain gradient results due to compressive strains on the lower part and tensile strains on the upper part. This strain gradient displaces local ions (Figure 2), which leads to a misalignment of the centers of gravities of positive (small circles) and negative (large circles) ions. This results in a net electric polarization in the direction indicated by the arrows.

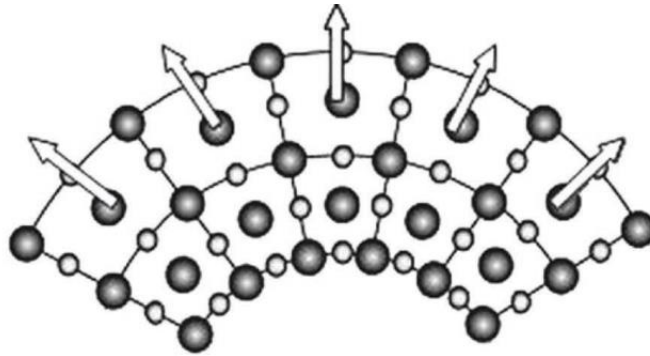


Figure 2: Misalignment of ions during bending [1]

Despite being a more general phenomenon than piezoelectricity, flexoelectricity was not observed in crystalline materials for a long time after its introduction in the 1960s. This is explained by the fact that without introducing permanent plastic deformation to a material, large strain gradients cannot be imparted in macroscopic materials. This is the case in high-performance piezoelectric crystals such as Lead Zirconate Titanate (PZT) and Barium Titanate (BT). In contrast, it is relatively easy to impart large uniform stress to these materials. Therefore, observing the piezoelectric effect is easier than the less evident flexoelectric effect. However, in smaller length scales, the effect of flexoelectricity is enhanced as it is possible for the materials to deform with large curvatures. Hence, in these materials, the size-dependent (macroscopic vs. microscopic) effect becomes more predominant.

1.2 FLEXOELECTRICITY IN SOFT MATERIALS

The mechanism of flexoelectricity in soft materials is not identical to hard materials, although the same naming convention is often used. Flexoelectricity has been proposed as the main effect in bulk soft materials, including liquid crystals, polymers and biomembranes.

The discovery of flexoelectricity in soft materials began with liquid crystals (LCs), which are soft materials and can flow like a liquid, yet still exhibit long-range crystalline order. LCs are known to exhibit piezoelectricity [3]. In 1969 Meyer proposed that the flexoelectric effect is also present in LCs and contributes to the electromechanical coupling. In LCs, flexoelectricity is explained on the basis of the asymmetric shape of polarized molecules. Flexoelectricity was first observed in the nematic LC phase. In this phase, polarized organics exhibit thread-like asymmetric (banana or pear) shapes and are self-aligned to display long-range ordering.

In aligned LCs the average orientation (director) is in the same direction. Each of the molecules is polarized, but the net polarization of the bulk is zero due to the random distribution of dipoles.

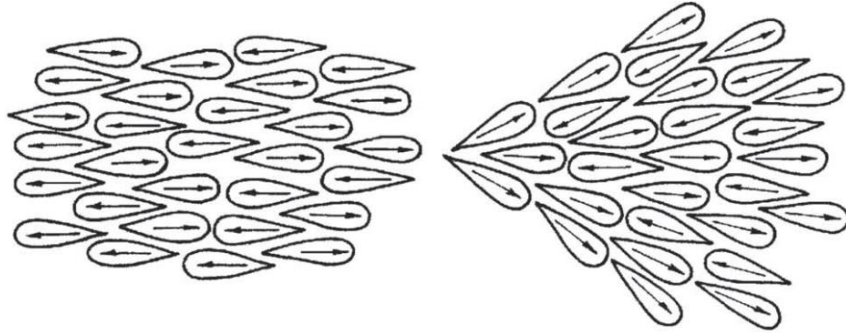


Figure 3: Calamitic phase - Pear/Rod-like LC molecules in normal (left) and splay deformation (right). Net polarization towards the right [1]

In splay (fan-like) deformation with the Calamitic (pear/rod-like) phase (Figure 3), the LCs undergo non-uniform deformation. This causes the molecules to reorient to an energetically favorable state. In this state, more dipoles are oriented in the same direction, which causes a net polarization across the bulk towards the right. With the Bent core (Banana-shaped) phase (Figure 4) under splay deformation, the net polarization across the bulk is towards the bottom.

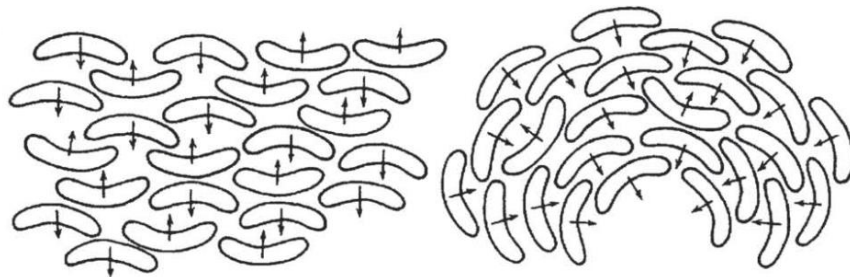


Figure 4: Bent-core phase - Banana-shaped LC molecules in normal (left) and splay deformation (right). Net polarization towards the bottom [1]

Therefore, the flexoelectric effect manifests as curvature induced polarization in liquid crystals. This effect becomes more significant in structures with larger curvature (smaller radius). In contrast to hard materials, in which flexoelectricity is generated by the relative displacement of negative and positive charge center, the basis of flexoelectricity in soft materials is the rotation of irregularly shaped polarized molecules. This is the key concept from Meyer's model (1969), and forms the basis for describing the flexoelectric effect in other soft material systems such as polymers and cellular membranes.

In Biology, the cell membrane is a fundamental unit of biological systems, comprising two main components: the cellular membrane and the cytoskeleton. The cell membrane is a lipid bilayer which can be considered a lipotropic phase LC [4]. The cytoskeleton forms the framework in which the other cell components such as the nucleus, mitochondria carry out their functions. As a LC, the cell membrane exhibits the flexoelectric effect. Both the direct and the converse flexoelectric effect have been observed in research conducted in artificial and natural cell membranes. The direct flexoelectric effect is the curvature-induced polarization, while the converse effect is the voltage-induced membrane curvature changes. Due to their small radius, systems at mesoscopic (atomic to micrometer) scales can exhibit significant flexoelectricity. [5,6]

The lipid bilayer molecules of the cell membrane are commonly modeled as a Calamitic phase (pear/rod-like cones) LC. In a flat bilayer lipid membrane, the polarized cones are randomly distributed across the membrane and as a result, there no net polarization across the membrane. When the membrane undergoes splay (bent) deformation (Figure 5), inner molecules reorient into energetically favorable states and generate a net dipole moment in the radial direction, which in turn generates an inner polarization. Therefore, the flexoelectric effect is generated in the cellular membrane by

the redistribution of the relative polarization orientations of the membrane lipid molecules under spherical deformation [1]. This is analogous to a strain gradient, but this mechanism is different from the flexoelectric effect in hard materials in which ions displace relative to one another.

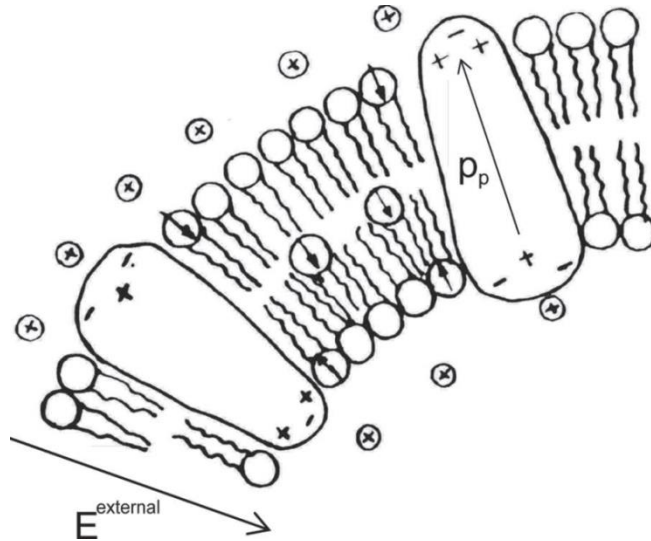


Figure 5: Bilayer lipid cell membrane [1]

1.3 A MODEL FOR OUTER HAIR CELL MEMBRANE

We focus now on a specific model for the cell membrane of the outer hair cells located in the inner ear. Brownell et al. [6] modeled the local stretching and contracting of these cells (called hair cells for the tiny hairs above the cells) by proposing that this stretching and contracting (called electromotility) was caused by the curvature changes in the membrane which are induced by the flexoelectric nature of the cell membrane. Figure 6 shows a cut-away view of the inner ear cell.

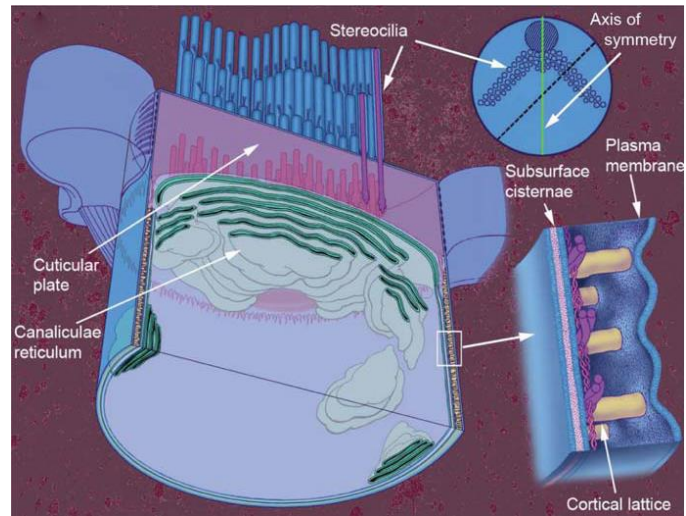


Figure 6: Inner ear hair cell. Figure on the right shows the cell membrane [24]

Brownell et al. modeled the cell membrane as a curved dielectric surface connected with a spring. The springs model the spectrin molecules which are embedded in the cortical lattice. Figure 7 shows the stretched and contracted hair cell. The horizontal links are spectrin molecules, while the links perpendicular to the spectrin molecules on the same plane are the actin filaments. Actin and spectrin are long chain protein polymers that provide a structural framework that maintains the shape of most cells.

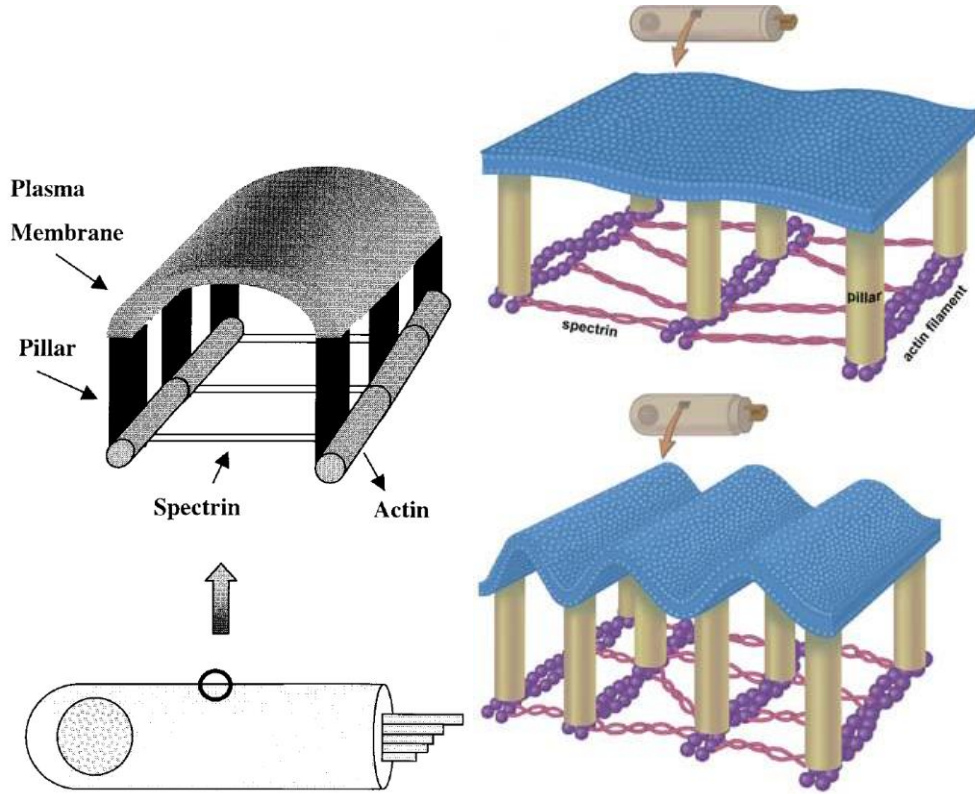


Figure 7: Inner ear cell membrane [6]

By calculating the total mechanical and electrical internal energy in the membrane, Brownell et al. found the total electric enthalpy per unit area.

$$\tilde{H} = \frac{1}{2}k_{eff}(c_1 - c_e)^2 - \frac{1}{2}h\epsilon_0E^2 - f\bar{c}E$$

Here, k_{eff} is the effective stiffness of the membrane and the spring (spectrin). c_1, c_e, \bar{c} are the curvature in the longitudinal direction, equilibrium curvature and average curvature, respectively. h is the membrane thickness, ϵ_0 is the permittivity of free space, E is the electric field and f is the flexoelectric coefficient with units of Coulombs. By taking the derivative of \tilde{H} with respect to c_1 and E they arrived at a set of linear equations for the moment, M , and the electric displacement, D_s , in the membrane, respectively.

$$M = \frac{\partial \tilde{H}}{\partial c_1} = k_{eff}(c_1 - c_e) - fE \quad (1.3)$$

$$D_s = -\frac{\partial \tilde{H}}{\partial E} = f\bar{c} + \varepsilon_0 hE \quad (1.4)$$

Brownell et al. also proposed a nonlinear total electric enthalpy using the Langevin function, $\mathcal{L}(\xi)$. The Langevin function gives the fraction of dipoles oriented in the direction of the applied field [6]. Using the Langevin function, they arrived at

$$\tilde{H} = \frac{1}{2}k_{eff}(c_1 - c_e)^2 - \frac{1}{2}h\varepsilon_0 E^2 - f_0\mathcal{L}(\xi)\bar{c}$$

By taking the same derivatives described in previous paragraph, they found a set of nonlinear equations to describe the moment and electric displacement in the membrane.

We note that the approach that Brownell et al. has taken could be further expanded. They chose to model the cell membrane as a dielectric surface which has mechanical and electric properties. The mechanical properties were modeled using basic solid mechanical assumptions, while the electrical properties assumed basic dielectric behavior.

Our goal is to formulate a nonlinear theory for flexoelectric membranes, which would reduce to a linear theory under certain conditions. We will revisit this model in Chapter 3.

Chapter 2: Formulation and Methodology

2.1 THERMODYNAMIC FORMULATION

To develop our formulation, we consider an incompressible dielectric membrane evenly sandwiched between two compliant electrodes as shown in Figure 8. The electrodes do not have any significant electrical resistance or mechanical stiffness. The membrane is subjected to in-plane forces and moments along its edges, as well as voltage.

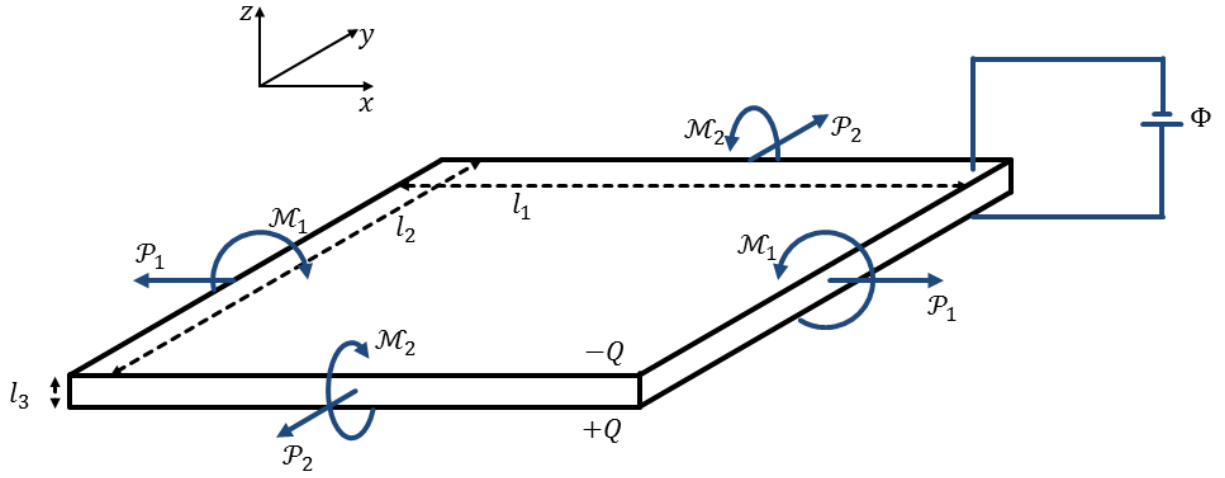


Figure 8: Schematic of dielectric membrane

This dielectric material is presumed to have the flexoelectric property. In the reference state, the membrane is not subjected to forces, moments or voltage. In this state, it has dimensions of L_1 , L_2 and L_3 . In the state shown on Figure 8, the membrane is subjected to in-plane forces \mathcal{P}_1 and \mathcal{P}_2 , and moments \mathcal{M}_1 and \mathcal{M}_2 . The electrodes are connected to a battery of voltage Φ . In this current state, the dimensions of the membrane become l_1 , l_2 and l_3 , while the two electrodes accumulate charges of $\pm Q$. To describe this membrane, we will use the in-plane stretches, the curvatures and the electric

displacement. The Helmholtz free energy density of the membrane (per unit area) is written as [7]

$$W = W(\lambda_1, \lambda_2, \kappa_1, \kappa_2, D) \quad (2.1)$$

Here, λ_1 and λ_2 denote the in-plane stretch, while κ_1 and κ_2 denote the curvature in the x and y directions. D denotes the electric displacement. The dependence of the Helmholtz free energy on κ_1 and κ_2 is inspired by classical plate theory [9]. The stretches are defined as $\lambda_1 = l_1/L_1$, $\lambda_2 = l_2/L_2$, and $\lambda_3 = l_3/L_3$. The electric field is defined as $E = \Phi/l_3$, while the electric displacement is defined as $D = Q/(l_1 l_2)$. The volume of the membrane is taken to remain unchanged during deformation. That is, the membrane is assumed to be incompressible so that

$$\lambda_1 \lambda_2 \lambda_3 = 1 \quad (2.2)$$

The potential energy of the applied loads (forces, moments and voltage) can be denoted by F and is given as

$$F = -\mathcal{P}_1 l_1 - \mathcal{P}_2 l_2 - \mathcal{M}_1 \kappa_1 l_1 - \mathcal{M}_2 \kappa_2 l_2 - \Phi Q$$

The membrane and the loads together constitute a thermodynamic system. We denote the free energy of this system by Π , and it consists of the Helmholtz free energy of the membrane along with the potential energy of the loads.

$$\Pi = W(\lambda_1, \lambda_2, \kappa_1, \kappa_2, D) l_1 l_2 + F$$

The Helmholtz free energy was multiplied by $l_1 l_2$ because we defined it as per unit area. When the forces, moments and voltage are fixed, the free energy of the system is a function of the five independent variables, $\Pi(\lambda_1, \lambda_2, \kappa_1, \kappa_2, D)$. The total free energy of the system is then

$$\begin{aligned} \Pi = & W(\lambda_1, \lambda_2, \kappa_1, \kappa_2, D) L_1 L_2 \lambda_1 \lambda_2 - \mathcal{P}_1 L_1 \lambda_1 - \mathcal{P}_2 L_2 \lambda_2 - \mathcal{M}_1 \kappa_1 L_1 \lambda_1 \\ & - \mathcal{M}_2 \kappa_2 L_2 \lambda_2 - \Phi L_1 L_2 \lambda_1 \lambda_2 D \end{aligned} \quad (2.3)$$

Minimizing the free energy of the system with respect to these variables determines the state of equilibrium.

$$\frac{\partial \Pi}{\partial \lambda_1} = \frac{\partial \Pi}{\partial \lambda_2} = \frac{\partial \Pi}{\partial \kappa_1} = \frac{\partial \Pi}{\partial \kappa_2} = \frac{\partial \Pi}{\partial D} = 0$$

Proceeding with $\frac{\partial \Pi}{\partial \lambda_1} = 0$,

$$\frac{\partial \Pi}{\partial \lambda_1} = \left(\lambda_1 \frac{\partial W}{\partial \lambda_1} + W \right) \lambda_2 L_1 L_2 - \mathcal{P}_1 L_1 - \mathcal{M}_1 \kappa_1 L_1 - \Phi L_1 L_2 \lambda_2 D = 0$$

We then divide the above equation by $l_1 l_2$, giving us

$$\left(\frac{\partial W}{\partial \lambda_1} + \frac{W}{\lambda_1} \right) - \frac{\mathcal{P}_1 L_1}{l_1 l_2} - \frac{\mathcal{M}_1 \kappa_1 L_1}{l_1 l_2} - \frac{\Phi L_1 L_2 \lambda_2 D}{l_1 l_2} = 0$$

Here, we define the in-plane forces per length as

$$p_1 = \frac{\mathcal{P}_1}{l_2}, p_2 = \frac{\mathcal{P}_2}{l_1}$$

The moments per length are similarly defined as

$$m_1 = \frac{\mathcal{M}_1}{l_2}, m_2 = \frac{\mathcal{M}_2}{l_1}$$

Then, we have that

$$\left(\frac{\partial W}{\partial \lambda_1} + \frac{W}{\lambda_1} \right) - \frac{p_1}{\lambda_1} - \frac{m_1 \kappa_1}{\lambda_1} - \frac{\Phi D}{\lambda_1} = 0$$

Multiplying through by λ_1 , we get

$$\lambda_1 \frac{\partial W}{\partial \lambda_1} + W = p_1 + m_1 \kappa_1 + \Phi D \quad (2.4)$$

For $\frac{\partial \Pi}{\partial \lambda_2} = 0$, we have, in a similar manner,

$$\lambda_2 \frac{\partial W}{\partial \lambda_2} + W = p_2 + m_2 \kappa_2 + \Phi D \quad (2.5)$$

Next, we proceed with $\frac{\partial \Pi}{\partial \kappa_1} = 0$, for which we find

$$\frac{\partial \Pi}{\partial \kappa_1} = L_1 L_2 \lambda_1 \lambda_2 \frac{\partial W}{\partial \kappa_1} - \mathcal{M}_1 L_1 \lambda_1 = 0$$

Dividing by $l_1 l_2$, we have

$$\frac{\partial W}{\partial \kappa_1} - \frac{\mathcal{M}_1 L_1 \lambda_1}{l_1 l_2} = 0$$

This reduces to the following.

$$\frac{\partial W}{\partial \kappa_1} = m_1 \quad (2.6)$$

Similarly, for $\frac{\partial \Pi}{\partial \kappa_2} = 0$, we have

$$\frac{\partial W}{\partial \kappa_2} = m_2 \quad (2.7)$$

Finally, proceeding with $\frac{\partial \Pi}{\partial D} = 0$, we have

$$\frac{\partial \Pi}{\partial D} = L_1 L_2 \lambda_1 \lambda_2 \frac{\partial W}{\partial D} - \Phi L_1 L_2 \lambda_1 \lambda_2 = 0$$

Again, dividing by $l_1 l_2$, we have

$$\frac{\partial W}{\partial D} = \Phi \quad (2.8)$$

Once the Helmholtz free energy function $W(\lambda_1, \lambda_2, \kappa_1, \kappa_2, D)$ is specified, equations (2.2), (2.4) – (2.8) constitute the equations of state. We note that equations (2.4) and (2.5) exhibit coupling between the in-plane forces and the moments, while equations (2.6) and (2.7) show no explicit coupling.

2.2 A FREE ENERGY FUNCTION

We are ready now to make certain assumptions about the free energy function. Here we assume that the membrane undergoes simple bending as shown in Figure 9. The kinematics are as follows.

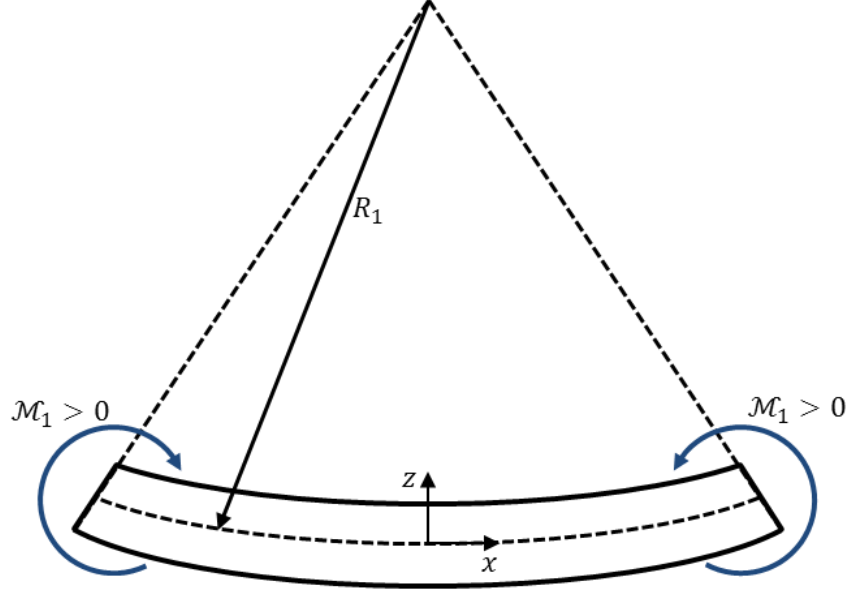


Figure 9: Schematic of membrane under simple bending with $\kappa_1 > 0$

Beginning with bending in the x -direction (κ_1), the strains in the x , y , and z (1, 2 and 3) direction, are

$$\varepsilon_1 = -\kappa_1 z, \quad \varepsilon_2 = \nu \kappa_1 z, \quad \varepsilon_3 = \nu \kappa_1 z$$

With bending in the y -direction (κ_2), we have that

$$\varepsilon_2 = -\kappa_2 z, \quad \varepsilon_1 = \nu \kappa_2 z, \quad \varepsilon_3 = \nu \kappa_2 z$$

Combining the strains from the two bending directions, the strains become

$$\varepsilon_1 = (\nu \kappa_2 - \kappa_1) z, \quad \varepsilon_2 = (\nu \kappa_1 - \kappa_2) z, \quad \varepsilon_3 = (\kappa_1 + \kappa_2) \nu z$$

We now consider only the effect of flexoelectricity, and disregard the effect of piezoelectricity. From equation (1.2) we had

$$P_i = \epsilon_0 \chi_{ij} E_j + \mu_{ijkl} \frac{\partial \varepsilon_{jk}}{\partial x_l}$$

Expanding the second term in the z (3) direction, we have

$$P_3^f = \mu_{3113} \frac{\partial \varepsilon_1}{\partial z} + \mu_{3223} \frac{\partial \varepsilon_2}{\partial z} + \mu_{3333} \frac{\partial \varepsilon_3}{\partial z}$$

Here, we've denoted the flexoelectric contribution to the polarization by P_3^f . Assuming that $\mu_{3113} = \mu_{3223} = \mu_1$ and $\mu_{3333} = \mu_2$ we have

$$P_3^f = \mu_1(\nu\kappa_2 - \kappa_1 + \nu\kappa_1 - \kappa_2) + \mu_2(\kappa_1 + \kappa_2)\nu$$

Collecting $(\kappa_1 + \kappa_2)$ terms, we have

$$P_3^f = [\mu_1(\nu - 1) + \mu_2\nu](\kappa_1 + \kappa_2)$$

Defining the effective flexoelectric coefficient as $\mu = \mu_1 - \nu(\mu_1 + \mu_2)$ and $\kappa = \kappa_1 + \kappa_2$ by assuming a transversely isotropic membrane, we obtain

$$P_3^f = -\mu\kappa \quad (2.9)$$

Hence, for $\kappa > 0$, we have $P_3^f < 0$ and vice-versa. This establishes our sign convention, which is consistent with other published conventions (See figure 1 and 2).

Figure 10 illustrates this convention.

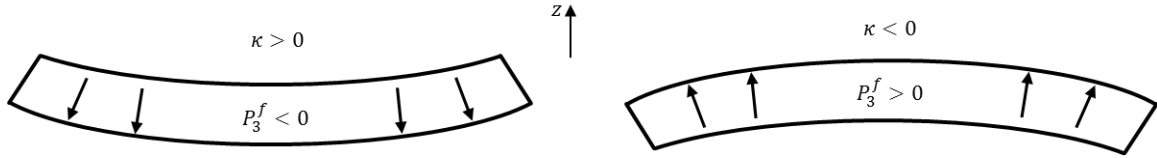


Figure 10: Schematic illustrating the sign convention for polarization and curvature

With dielectric and flexoelectric effects, the polarization in the z (3) direction becomes

$$P_3 = \epsilon_0\chi E_3 - \mu\kappa \quad (2.10)$$

Next, we focus our attention on the electric displacement. The electric displacement is given by

$$D_i = \epsilon_0 E_i + P_i \quad (2.11)$$

In the z (3) direction equation (2.11) becomes

$$D_3 = \epsilon_0 E_3 + P_3$$

Using equation (2.10), we have

$$D_3 = \epsilon_0 E_3 + \epsilon_0 \chi E_3 - \mu \kappa$$

$$D_3 = (\epsilon_0 + \epsilon_0 \chi) E_3 - \mu \kappa; \epsilon = \epsilon_0 (1 + \chi)$$

Here, ϵ is the permittivity of the membrane and $(1 + \chi)$ is the relative permittivity.

Dropping the subscripts, we have,

$$D = \epsilon E - \mu \kappa \quad (2.12)$$

Next, solving for E from the above equation, we get

$$E = \frac{1}{\epsilon} (D + \mu \kappa)$$

Using $E = \Phi/l_3$, and equation (2.8), we have that

$$\frac{\partial W}{\partial D} = \Phi = \frac{l_3}{\epsilon} (D + \mu \kappa) \quad (2.13)$$

We then integrate the above equation with respect to D , and find

$$W = \frac{l_3}{2\epsilon} D^2 + \frac{\mu l_3}{\epsilon} \kappa D + W_{sb}(\lambda_1, \lambda_2, \kappa_1, \kappa_2) \quad (2.14)$$

At this point, we have specified the flexoelectric contribution to the Helmholtz free energy. The last term in the above equation is the free energy density associated with stretching and bending, which will be specified in the next section.

Returning to the free energy of the system from equation (2.3), we now have

$$\begin{aligned} \Pi = & L_1 L_2 \lambda_1 \lambda_2 W_{sb} + L_1 L_2 L_3 \left(\frac{D^2}{2\epsilon} + \frac{\mu \kappa D}{\epsilon} \right) - \mathcal{P}_1 L_1 \lambda_1 - \mathcal{P}_2 L_2 \lambda_2 - \mathcal{M}_1 \kappa_1 L_1 \lambda_1 \\ & - \mathcal{M}_2 \kappa_2 L_2 \lambda_2 - \frac{L_1 L_2 L_3}{\epsilon} D (D + \mu \kappa) \end{aligned}$$

This expression simplifies to

$$\Pi = L_1 L_2 \lambda_1 \lambda_2 W_{sb} - \mathcal{P}_1 L_1 \lambda_1 - \mathcal{P}_2 L_2 \lambda_2 - \mathcal{M}_1 \kappa_1 L_1 \lambda_1 - \mathcal{M}_2 \kappa_2 L_2 \lambda_2 - \frac{L_1 L_2 L_3}{2\epsilon} D^2$$

Then, substituting $D = \epsilon E - \mu \kappa$, the free energy of the system becomes

$$\begin{aligned} \Pi = & L_1 L_2 \lambda_1 \lambda_2 W_{sb} - \mathcal{P}_1 L_1 \lambda_1 - \mathcal{P}_2 L_2 \lambda_2 - \mathcal{M}_1 \kappa_1 L_1 \lambda_1 - \mathcal{M}_2 \kappa_2 L_2 \lambda_2 \\ & - \frac{L_1 L_2 L_3}{2\epsilon} \left(\frac{\epsilon \Phi}{L_3} \lambda_1 \lambda_2 - \mu \kappa \right)^2 \end{aligned} \quad (2.15)$$

We now perform an analysis similar to section 2.1. Beginning with the expression for $\frac{\partial \Pi}{\partial \lambda_1} = 0$, we have

$$\frac{\partial \Pi}{\partial \lambda_1} = \left(\lambda_1 \frac{\partial W_{sb}}{\partial \lambda_1} + W_{sb} \right) L_1 L_2 \lambda_2 - \mathcal{P}_1 L_1 - \mathcal{M}_1 \kappa_1 L_1 - \Phi L_1 L_2 \lambda_2 \left(\frac{\epsilon \Phi}{L_3} \lambda_1 \lambda_2 - \mu \kappa \right) = 0$$

Dividing the above equation by $l_1 l_2$, we have

$$\left(\frac{\partial W_{sb}}{\partial \lambda_1} + \frac{W_{sb}}{\lambda_1} \right) - \frac{\mathcal{P}_1 L_1}{l_1 l_2} - \frac{\mathcal{M}_1 \kappa_1 L_1}{l_1 l_2} - \frac{\Phi L_1 L_2 \lambda_2}{l_1 l_2} \left(\frac{\epsilon \Phi}{L_3} \lambda_1 \lambda_2 - \mu \kappa \right) = 0$$

Using the in-plane forces per length and moments per length, we have

$$\left(\frac{\partial W_{sb}}{\partial \lambda_1} + \frac{W_{sb}}{\lambda_1} \right) - \frac{p_1}{\lambda_1} - \frac{m_1 \kappa_1}{\lambda_1} - \frac{\Phi}{\lambda_1} \left(\frac{\epsilon \Phi}{L_3} \lambda_1 \lambda_2 - \mu \kappa \right) = 0$$

Finally, multiplying by λ_1 , we have

$$\lambda_1 \frac{\partial W_{sb}}{\partial \lambda_1} + W_{sb} = p_1 + m_1 \kappa_1 + \frac{\epsilon \Phi^2}{L_3} \lambda_1 \lambda_2 - \mu \kappa \Phi \quad (2.16)$$

Similarly for $\frac{\partial \Pi}{\partial \lambda_2} = 0$, we have

$$\lambda_2 \frac{\partial W_{sb}}{\partial \lambda_2} + W_{sb} = p_2 + m_2 \kappa_2 + \frac{\epsilon \Phi^2}{L_3} \lambda_1 \lambda_2 - \mu \kappa \Phi \quad (2.17)$$

For $\frac{\partial \Pi}{\partial \kappa_1} = 0$, we have

$$\frac{\partial \Pi}{\partial \kappa_1} = L_1 L_2 \lambda_1 \lambda_2 \frac{\partial W_{sb}}{\partial \kappa_1} - \mathcal{M}_1 L_1 \lambda_1 + \frac{L_1 L_2 L_3}{\epsilon} \mu \left(\frac{\epsilon \Phi}{L_3} \lambda_1 \lambda_2 - \mu \kappa \right) = 0$$

Dividing the above equation by $l_1 l_2$, we have

$$\frac{\partial W_{sb}}{\partial \kappa_1} - \frac{\mathcal{M}_1 L_1 \lambda_1}{l_1 l_2} + \frac{L_1 L_2 L_3}{\epsilon l_1 l_2} \mu \left(\frac{\epsilon \Phi}{L_3} \lambda_1 \lambda_2 - \mu \kappa \right) = 0$$

Using the in-plane forces per length and moments per length, we have

$$\begin{aligned} \frac{\partial W_{sb}}{\partial \kappa_1} - m_1 + \frac{L_3 \mu}{\epsilon \lambda_1 \lambda_2} \left(\frac{\epsilon \Phi}{L_3} \lambda_1 \lambda_2 - \mu \kappa \right) &= 0 \\ \frac{\partial W_{sb}}{\partial \kappa_1} &= m_1 - \mu \Phi + \frac{L_3 \mu^2 \kappa}{\epsilon \lambda_1 \lambda_2} \end{aligned}$$

Expanding the $\mu \Phi$ term by using $\Phi = l_3 / \epsilon (D + \mu \kappa)$, we finally get

$$\frac{\partial W_{sb}}{\partial \kappa_1} = m_1 - \frac{\mu L_3}{\epsilon} \frac{D}{\lambda_1 \lambda_2} \quad (2.18)$$

Similarly for $\frac{\partial \Pi}{\partial \kappa_2} = 0$, we have

$$\frac{\partial W_{sb}}{\partial \kappa_2} = m_2 - \frac{\mu L_3}{\epsilon} \frac{D}{\lambda_1 \lambda_2} \quad (2.19)$$

Next, we write the physical quantities - Φ , p_1 , p_2 , m_1 , m_2 - in terms of the state variables - D , λ_1 , λ_2 , κ_1 , κ_2 . From equations (2.13), (2.18) and (2.19), the physical quantities Φ , m_1 , m_2 become

$$\Phi = \frac{L_3}{\epsilon \lambda_1 \lambda_2} (D + \mu \kappa) \quad (2.20)$$

$$m_1 = \frac{\partial W_{sb}}{\partial \kappa_1} + \frac{\mu L_3}{\epsilon} \frac{D}{\lambda_1 \lambda_2} \quad (2.21)$$

$$m_2 = \frac{\partial W_{sb}}{\partial \kappa_2} + \frac{\mu L_3}{\epsilon} \frac{D}{\lambda_1 \lambda_2} \quad (2.22)$$

For the quantities p_1 , p_2 , some manipulation and substitution is required. From equation (2.16), the physical quantity p_1 becomes

$$p_1 = \lambda_1 \frac{\partial W_{sb}}{\partial \lambda_1} + W_{sb} - m_1 \kappa_1 - \frac{\epsilon \Phi^2}{L_3} \lambda_1 \lambda_2 + \mu \kappa \Phi$$

Next, we use equation (2.20) and equation (2.21) and arrive at

$$p_1 = \lambda_1 \frac{\partial W_{sb}}{\partial \lambda_1} + W_{sb} - \left(\frac{\partial W_{sb}}{\partial \kappa_1} + \frac{\mu L_3}{\epsilon} \frac{D}{\lambda_1 \lambda_2} \right) \kappa_1 - \frac{\epsilon}{L_3} \lambda_1 \lambda_2 \left(\frac{l_3}{\epsilon} \right)^2 (D + \mu \kappa)^2 + \mu \kappa \frac{l_3}{\epsilon} (D + \mu \kappa)$$

Expanding the terms, we find

$$p_1 = \lambda_1 \frac{\partial W_{sb}}{\partial \lambda_1} + W_{sb} - \kappa_1 \frac{\partial W_{sb}}{\partial \kappa_1} - \frac{\mu l_3 \kappa_1}{\epsilon} D - \frac{l_3}{\epsilon} (D^2 + 2\mu D \kappa + \mu^2 \kappa^2) + \frac{l_3}{\epsilon} (\mu D \kappa + \mu^2 \kappa^2)$$

We then combine like-terms from the last three terms and use $\kappa = \kappa_1 + \kappa_2$ to find

$$p_1 = \lambda_1 \frac{\partial W_{sb}}{\partial \lambda_1} + W_{sb} - \kappa_1 \frac{\partial W_{sb}}{\partial \kappa_1} - \frac{\mu l_3 \kappa_1}{\epsilon} D - \frac{l_3}{\epsilon} (D^2 + \mu D (\kappa_1 + \kappa_2))$$

Finally, we use $l_3 = L_3 / \lambda_1 \lambda_2$ and combine the remaining like-terms to arrive at

$$p_1 = \lambda_1 \frac{\partial W_{sb}}{\partial \lambda_1} + W_{sb} - \kappa_1 \frac{\partial W_{sb}}{\partial \kappa_1} - \frac{L_3}{\epsilon} \frac{D^2}{\lambda_1 \lambda_2} - \frac{\mu L_3}{\epsilon} \frac{D}{\lambda_1 \lambda_2} (2\kappa_1 + \kappa_2) \quad (2.23)$$

Similarly for p_2 , we have

$$p_2 = \lambda_2 \frac{\partial W_{sb}}{\partial \lambda_2} + W_{sb} - \kappa_2 \frac{\partial W_{sb}}{\partial \kappa_2} - \frac{L_3}{\epsilon} \frac{D^2}{\lambda_1 \lambda_2} - \frac{\mu L_3}{\epsilon} \frac{D}{\lambda_1 \lambda_2} (\kappa_1 + 2\kappa_2) \quad (2.24)$$

2.3 SMALL-STRAIN FORMULATION

Having expressed the physical quantities in terms of the state variables, we are now ready to define the free energy related to stretching and bending. Beginning with the free energy for stretching, we look at Gent's free energy [8] for stretching defined per volume:

$$W_s(\lambda_1, \lambda_2) = -\frac{GJ_{lim}}{2} \log \left(1 - \frac{\lambda_1^2 + \lambda_2^2 + \lambda_1^{-2} \lambda_2^{-2} - 3}{J_{lim}} \right)$$

Here, G is the small-stress shear modulus and J_{lim} is a dimensionless parameter related to the limiting stretch. At this point, we attempt to simplify the problem by assuming small strains. Using $\lambda_1 = \epsilon_1 + 1$ and $\lambda_2 = \epsilon_2 + 1$, and expanding using Taylor Series, we arrive at

$$W_s(\epsilon_1, \epsilon_2) = 2G(\epsilon_1^2 + \epsilon_2^2 + \epsilon_1 \epsilon_2)$$

Note that this assumes plane stress and incompressibility. It can be shown that with this free energy function, the plane stress relations of σ vs. ϵ can be retrieved. In addition, this free energy is defined per unit volume. The free energy per unit area would be

$$\overline{W}_s(\epsilon_1, \epsilon_2) = W_s(\epsilon_1, \epsilon_2) l_3$$

With the small-strain assumption, $l_3 \approx L_3$, so that

$$\overline{W}_s(\epsilon_1, \epsilon_2) = W_s(\epsilon_1, \epsilon_2) L_3$$

Thus, the free energy related to stretching becomes

$$\overline{W}_s(\epsilon_1, \epsilon_2) = 2L_3 G(\epsilon_1^2 + \epsilon_2^2 + \epsilon_1 \epsilon_2) \quad (2.25)$$

Next, we look at the free energy related to bending per unit area. From classical plate theory [9], we find

$$W_b(\kappa_1, \kappa_2) = \frac{\tilde{D}}{2} [(\kappa_1 + \kappa_2)^2 - 2(1 - \nu)\kappa_1\kappa_2] \quad (2.26)$$

Here $\tilde{D} = \frac{EL_3^3}{12(1-\nu^2)}$ is the flexural rigidity, and Poisson's ratio is $\nu = 0.5$ for a soft, elastomeric membrane. With $E = 2G(1 + \nu) = 3G$, we have that $\tilde{D} = \frac{GL_3^3}{3}$. Note that $l_3 \approx L_3 = \text{const.}$ for small-strain assumption. We note that this free energy resembles the Helfrich free energy for membranes. Thus, the free energy for stretching and bending, W_{sb} , is given by

$$\begin{aligned} W_{sb}(\varepsilon_1, \varepsilon_2, \kappa_1, \kappa_2) &= \overline{W}_s(\varepsilon_1, \varepsilon_2) + W_b(\kappa_1, \kappa_2) \\ W_{sb}(\varepsilon_1, \varepsilon_2, \kappa_1, \kappa_2) &= 2L_3G(\varepsilon_1^2 + \varepsilon_2^2 + \varepsilon_1\varepsilon_2) + \frac{\tilde{D}}{2} [(\kappa_1 + \kappa_2)^2 - \kappa_1\kappa_2] \end{aligned} \quad (2.27)$$

Now we are ready to express the Helmholtz free energy for our formulation. From (2.27) and (2.14), we have

$$W = \frac{L_3}{2\varepsilon} D^2 + \frac{\mu L_3}{\varepsilon} \kappa D + 2L_3G(\varepsilon_1^2 + \varepsilon_2^2 + \varepsilon_1\varepsilon_2) + \frac{\tilde{D}}{2} [(\kappa_1 + \kappa_2)^2 - \kappa_1\kappa_2] \quad (2.28)$$

The first two terms in equation (2.28) represent the flexoelectric assumptions we made about the material. The last two terms represent the free energy for stretching and bending. We note that W must be positive-definite, and resolve the issues that arise from a non-positive-definite free energy function in section 2.4

Having obtained the expression for the free energy related to stretching and bending, we can use the small strain assumptions that $l_3 \approx L_3$, $\lambda_1\lambda_2 \approx 1$, and that $\frac{\partial W_{sb}}{\partial \lambda_1} = \frac{\partial W_{sb}}{\partial \varepsilon_1}$ since $\varepsilon_1 = \lambda_1 - 1$, and $\frac{\partial W_{sb}}{\partial \lambda_2} = \frac{\partial W_{sb}}{\partial \varepsilon_2}$ since $\varepsilon_2 = \lambda_2 - 1$, to simplify equations (2.20) – (2.24). We first evaluate the following derivatives which appear in those equations.

$$\begin{aligned} \frac{\partial W_{sb}}{\partial \varepsilon_1} &= 2L_3G(2\varepsilon_1 + \varepsilon_2) \\ \frac{\partial W_{sb}}{\partial \varepsilon_2} &= 2L_3G(2\varepsilon_2 + \varepsilon_1) \\ \frac{\partial W_{sb}}{\partial \kappa_1} &= \tilde{D}[\kappa_1 + \frac{1}{2}\kappa_2] \end{aligned}$$

$$\frac{\partial W_{sb}}{\partial \kappa_2} = \tilde{D} \left[\kappa_2 + \frac{1}{2} \kappa_1 \right]$$

Hence, equations (2.20) – (2.22) become

$$\Phi = \frac{L_3}{\epsilon} (D + \mu \kappa) \quad (2.29)$$

$$m_1 = \tilde{D} \left[\kappa_1 + \frac{1}{2} \kappa_2 \right] + \frac{\mu L_3}{\epsilon} D \quad (2.30)$$

$$m_2 = \tilde{D} \left[\kappa_2 + \frac{1}{2} \kappa_1 \right] + \frac{\mu L_3}{\epsilon} D \quad (2.31)$$

For equation (2.23), we have

$$\begin{aligned} p_1 = & 2L_3 G(2\varepsilon_1 + \varepsilon_2) + 2L_3 G(\varepsilon_1^2 + \varepsilon_2^2 + \varepsilon_1 \varepsilon_2) + \frac{\tilde{D}}{2} [(\kappa_1 + \kappa_2)^2 - \kappa_1 \kappa_2] \\ & - \kappa_1 \left(\tilde{D} \left[\kappa_1 + \frac{1}{2} \kappa_2 \right] \right) - \frac{L_3}{\epsilon} D^2 - \frac{\mu L_3}{\epsilon} D(2\kappa_1 + \kappa_2) \end{aligned}$$

Neglecting all 2nd order terms in strain and curvature, we have

$$p_1 = 2L_3 G(2\varepsilon_1 + \varepsilon_2) - \frac{L_3}{\epsilon} D^2 - \frac{\mu L_3}{\epsilon} D(2\kappa_1 + \kappa_2) \quad (2.32)$$

Finally for equation (2.24), we have

$$p_2 = 2L_3 G(2\varepsilon_2 + \varepsilon_1) - \frac{L_3}{\epsilon} D^2 - \frac{\mu L_3}{\epsilon} D(\kappa_1 + 2\kappa_2) \quad (2.33)$$

It is important to note that the flexoelectric effect is reflected in equations (2.29) – (2.33) by the additional terms containing the flexoelectric coefficient, μ . In equation (2.32) and (2.33), for example, the first term is a form of the known stress-strain relationship, the second term is the so-called Maxwell stress, and the final term is the flexoelectric term.

2.4 LIMITATIONS OF THE FREE ENERGY FUNCTION

In this section, we will examine the Helmholtz free energy function in closer detail. From equation (2.28) we had

$$W = \frac{L_3}{2\epsilon} D^2 + \frac{\mu L_3}{\epsilon} \kappa D + 2L_3 G(\epsilon_1^2 + \epsilon_2^2 + \epsilon_1 \epsilon_2) + \frac{\tilde{D}}{2} [(\kappa_1 + \kappa_2)^2 - \kappa_1 \kappa_2]$$

With the assumption of plane-strain bending, that is $\epsilon_1 = \epsilon_2 = 0$ and $\kappa_2 = 0$, we find

$$W(\kappa, D) = \frac{L_3}{2\epsilon} D^2 + \frac{\mu L_3}{\epsilon} \kappa D + \frac{\tilde{D}}{2} \kappa^2 \quad (2.34)$$

For W to be positive definite, it is required that the discriminant, Δ , of the quadratic function be less than zero. Hence, for equation (2.34)

$$\Delta = \left(\frac{\mu L_3}{\epsilon}\right)^2 - 4\left(\frac{\tilde{D}}{2}\right)\left(\frac{L_3}{2\epsilon}\right) < 0 \quad (2.35)$$

Upon expansion and simplification, equation (2.35) reduces to

$$\left(\tilde{D} - \frac{L_3 \mu^2}{\epsilon}\right) > 0 \quad (2.36)$$

We define the term in parenthesis in (2.36) as the effective flexural rigidity given by

$$\tilde{D}_{eff} = \tilde{D} - \frac{L_3 \mu^2}{\epsilon} \quad (2.37)$$

Hence, (2.36) becomes

$$L_3 \left(\frac{GL_3^2}{3} - \frac{\mu^2}{\epsilon}\right) > 0$$

This implies that

$$L_3 > \sqrt{\frac{3\mu^2}{G\epsilon}}$$

Therefore, for a positive definite Helmholtz free energy, W , the effective flexural rigidity of the membrane must be greater than zero. This results in the requirement that the membrane thickness L_3 must be greater than a critical thickness, L_c where

$$L_c = \sqrt{\frac{3\mu^2}{G\epsilon}} \quad (2.38)$$

Table 1 lists the value of the critical thickness for certain soft materials and ceramics.

Table 1: Values of critical thickness, L_c , for common soft and hard materials

Soft materials: Polymers and Elastomers				
Flexoelectricity magnitude	Flexoelectric Coefficient $\left(\frac{C}{m}\right)$	Young's Modulus $\left(\frac{N}{m^2}\right)$	Permittivity $\left(\frac{C^2}{Nm^2}\right)$	L_c (m)
Minimum FC	0.000000013	14000000	1.77082E-11	2.47693E-06
Maximum FC	0.00008	52000000000	8.8541E-11	0.00011185
Minimum FC	0.000000013	52000000000	8.8541E-11	1.81757E-08
Maximum FC	0.00008	14000000	1.77082E-11	0.015242634
Ceramics				
Material type	Flexoelectric Coefficient $\left(\frac{C}{m}\right)$	Young's Modulus $\left(\frac{N}{m^2}\right)$, average value	Electric Permittivity $\left(\frac{C^2}{Nm^2}\right)$, commonly $\left(\frac{F}{m}\right)$	L_c (m)
BaTiO3	0.00005	3.5E+11	8.85507E-08	8.52042E-07
Ba0.67Sr0.33TiO3	0.000123333	3.5E+11	1.59384E-07	1.56655E-06
Ba0.65Sr0.35TiO3	0.0000085	3.5E+11	3.6311E-08	2.26197E-07
PbMg0.33Nb0.67O3	0.0000035	3.5E+11	1.15113E-07	5.23109E-08
PMN-PT	0.000022	3.5E+11	1.85947E-07	2.58711E-07
Pb0.3Sr0.7TiO3	0.00002	3.5E+11	1.1954E-07	2.93332E-07
Pb(Zr,Ti)O3	0.00000095	3.5E+11	1.94881E-08	3.45085E-08

It is important to note that in soft materials with large flexoelectric coefficients, the critical thickness is significantly large. Yet, there is disagreement among researchers regarding the values of flexoelectric coefficients for soft materials [12], [21] – [23]. In addition to disagreement with the values of the flexoelectric coefficient, there is also inconsistency in the dimensions of the flexoelectric coefficient. We have used μ with dimensions of $\frac{Charge}{length}$, typically $\frac{C}{m}$, while others have used $f = \frac{\mu}{\epsilon}$ with units of *Volts, V*. There are also those who have used $f = \mu L_3$ with units of *C*.

2.5 A SANDWICH MODEL

In order to resolve the issue of non-positive definite W for $L_3 < L_c$, we propose the following sandwich model. We consider the membrane to be sandwiched between two elastic electrode layers. The layers have a shear modulus of G_2 and a thickness of t , while the membrane has a shear modulus of G_1 , as shown in Figure 11.

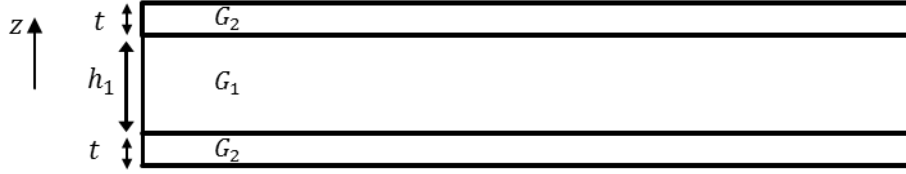


Figure 11: Schematic of the sandwich model

From inequality (2.36), the effective flexural rigidity of the sandwich, \tilde{D}_{eff} , consists of the flexural rigidity of the composite, \tilde{D}_{comp} (membrane plus top and bottom layers) less the corrective term due to the flexoelectric property of the membrane.

$$\tilde{D}_{eff} = \tilde{D}_{comp} - \frac{h_1 \mu^2}{\epsilon}$$

Note that we have switched from L_3 to h_1 for the membrane thickness for convenience. As per (2.36), for a positive-definite W , we require that the effective flexural rigidity be greater than zero. The flexural rigidity of the composite is given by

$$\tilde{D}_{comp} = \frac{G_1 h_1^3}{3} + \frac{G_2}{3} [(h_1 + 2t)^3 - h_1^3]$$

Here we have used $\nu = 0.5$ for soft, elastomeric materials. After expanding and collecting like terms, we arrive at the following expression for \tilde{D}_{eff} .

$$\tilde{D}_{eff} = \left(\frac{G_1}{3}\right) h_1^3 + (2G_2 t) h_1^2 + \left(4G_2 t^2 - \frac{\mu^2}{\epsilon}\right) h_1 + \frac{8}{3} G_2 t^3 \quad (2.39)$$

To simplify our analysis, we normalize equation (2.39) by $G_1 L_c^3$. Doing so, we find

$$\overline{\overline{D_{eff}}} = \frac{1}{3}\overline{h_1}^3 + (2\overline{G}\overline{t})\overline{h_1}^2 + \left(4\overline{G}\overline{t}^2 - \frac{1}{3}\right)\overline{h_1} + \frac{8}{3}\overline{G}\overline{t}^3 \quad (2.40)$$

Here we have that

$$\overline{\overline{D_{eff}}} = \frac{\tilde{D}_{eff}}{G_1 L_c^3}; \overline{h_1} = \frac{h_1}{L_c}; \overline{t} = \frac{t}{L_c}; \overline{G} = \frac{G_2}{G_1}$$

Taking the derivative of $\overline{\overline{D_{eff}}}$ with respect to $\overline{h_1}$ we find

$$\frac{d\overline{\overline{D_{eff}}}}{d\overline{h_1}} = \overline{h_1}^2 + (4\overline{G}\overline{t})\overline{h_1} + \left(4\overline{G}\overline{t}^2 - \frac{1}{3}\right) \quad (2.41)$$

In order to ensure that $\overline{\overline{D_{eff}}}$ remains greater than zero for $\overline{h_1}$ greater than zero, the last term in equation (2.41) (the y-intercept) must be greater than zero. Hence,

$$4\overline{G}\overline{t}^2 - \frac{1}{3} > 0$$

This leads to

$$\overline{t} > \frac{1}{2\sqrt{3\overline{G}}}$$

Or that

$$\overline{t}_c = \frac{1}{2\sqrt{3\overline{G}}}$$

Therefore, to ensure that we have a positive-definite Helmholtz free energy, W , for the sandwich model, there is a critical thickness, t_c , for the top and bottom layers of the sandwich for which $t > t_c$ results in a positive-definite W . To arrive at an expression for t_c , we note that $t_c = L_c \overline{t}_c$. Hence,

$$t_c = \frac{1}{2} \sqrt{\frac{\mu^2}{G_2 \epsilon}} \quad (2.42)$$

It is interesting to note that the critical thickness of the top and bottom layers of the sandwich depends of the mechanical property of the top and bottom layers (G_2 , shear modulus of the layers) while also depending on the flexoelectric and dielectric properties (μ, ϵ) of the membrane being sandwiched.

Next, we plot the normalized effective flexural rigidity ($\overline{\widetilde{D}_{eff}}$) against the normalized membrane thickness ($\overline{h_1}$). We use $\overline{G} = 4$, (for which $\overline{t}_c = \frac{1}{4\sqrt{3}} = 0.1443$) and increasing values of \overline{t} . For $\overline{t} > \overline{t}_c$, we note that $\overline{\widetilde{D}_{eff}}$ is greater than zero, ensuring a positive-definite Helmholtz free energy, W . Figure 12 shows the results.

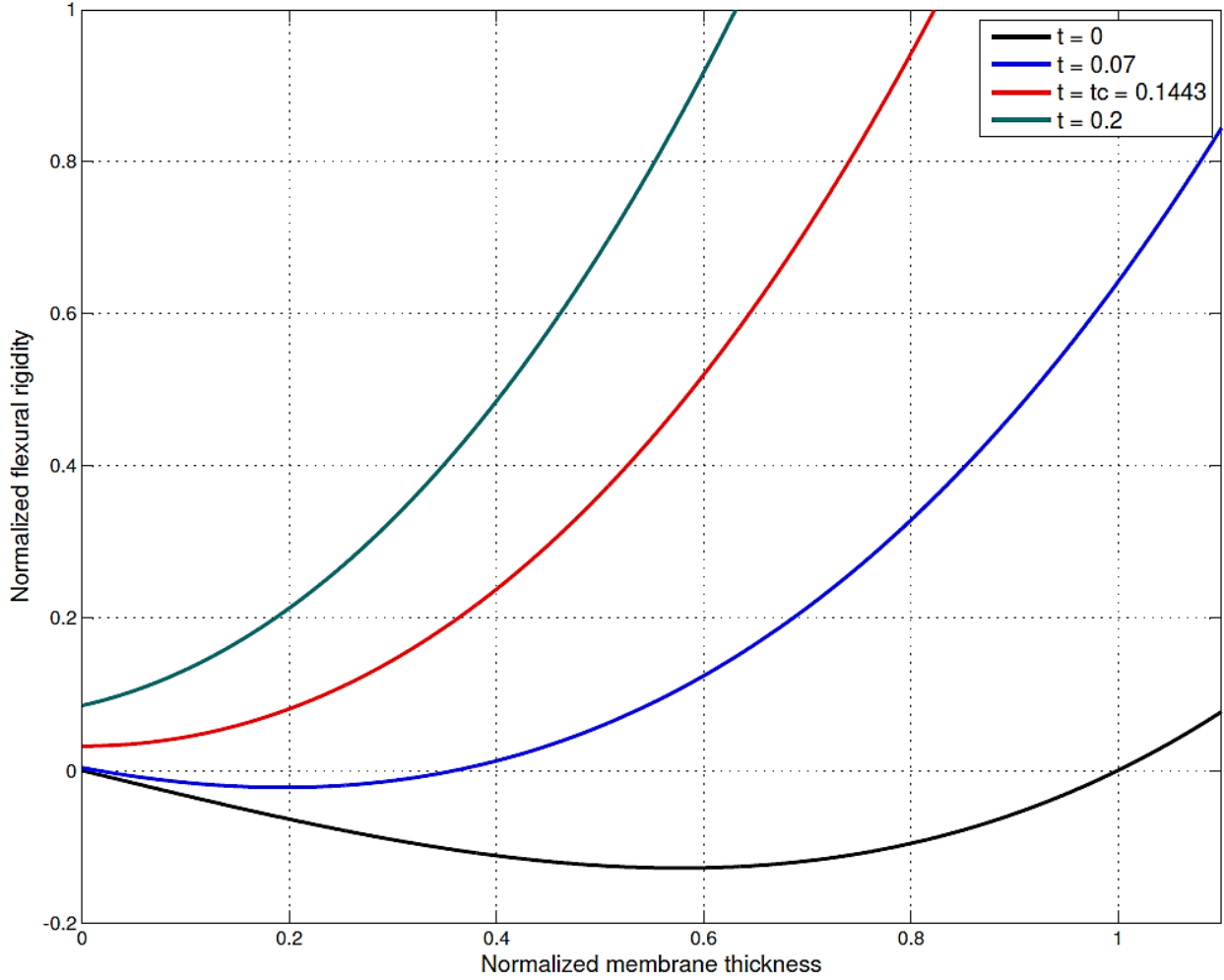


Figure 12: Normalized effective flexural rigidity versus normalized membrane thickness

Chapter 3: Results and Discussions

3.1 FLEXOELECTRIC COEFFICIENT MEASUREMENTS

In order to determine the effectiveness of the equations that were derived in the previous section, experimental efforts to measure the flexoelectric coefficient of certain ceramic materials are studied in this section. The major experimental technique for measuring the flexoelectric coefficient was developed by Cross et al. in 2001 [10] on $\text{Pb}(\text{Mg}_{1/3}\text{Nb}_{2/3})\text{O}_3$ (PMN) ferroelectric perovskite sample. Additional experiments have been performed by Cross et al. [13-17] which have taken additional effects into consideration (temperature, for example), but the basic setup of the experiment has remained the same. Later on in 2012 Baskaran et al. performed a similar experiment on α -phase PVDF film.

We will attempt to use the experimental data gathered by Cross et al. and Baskaran et al. to arrive at flexoelectric coefficient values by using equations (2.29) – (2.33) derived in the previous chapter. Below is a detailed explanation of the steps taken to compare flexoelectric coefficient values.

Cross et al. (2001) method for measuring the flexoelectric coefficient [10]

In this paper [10] and in following papers, [13-17] Cross et al. used the basic experimental setup shown in figure 13, with some modifications to accommodate for other factors, like temperature.

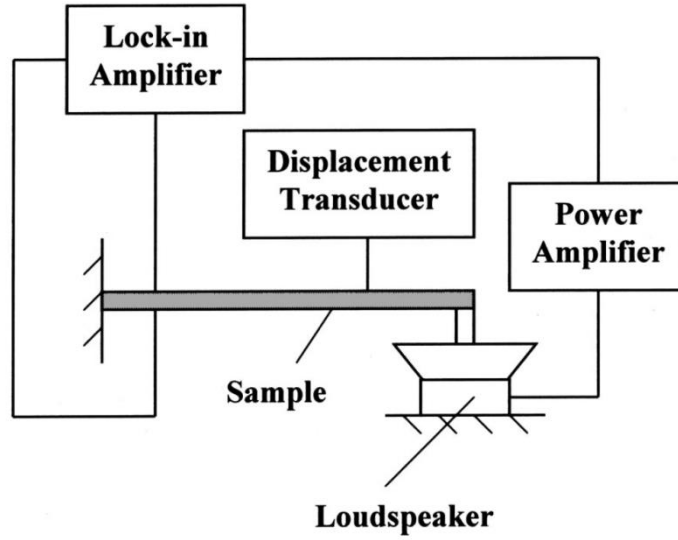


Figure 13: Experimental setup by Cross et al. for measurement of flexoelectric coefficient [10]

Sample:

$\text{Pb}(\text{Mg}_{1/3}\text{Nb}_{2/3})\text{O}_3$ (PMN) ferroelectric perovskite of 76.3 mm length (L), 12.7 mm width and 2.5 mm thickness.

Approach:

A very thin layer of sputtered gold was used as an electrode. The bottom surface of the sample is fully covered with gold while the top surface has a series of 3mm diameter electrodes. The sample is cantilevered at one end. At the opposite end, a loudspeaker was used to displace the sample at a frequency of 1 Hz.

At two locations along the bar ($\bar{x} = \frac{x}{L} = 0.18$ and $\bar{x} = \frac{x}{L} = 0.67$) measurements were taken of the vertical displacement, w , and the current, i . There were 10 measurements taken at each of the two locations, with the power of the loudspeaker increased in each measurement.

The polarization was then calculated using the following equation.

$$P_3 = \frac{i}{2\pi f A} \quad (3.1)$$

Here, f is the frequency, and A is electrode area. The polarization due to flexoelectricity is given by

$$P_3 = \mu_{12} \frac{\partial \epsilon_{11}}{\partial x_3} \quad (3.2)$$

In order to find the flexoelectric coefficient, Cross et al. plotted the polarization verses the strain gradient. The flexoelectric coefficient would then be found as the slope of the linear curve. The strain gradient, $\frac{\partial \epsilon_{11}}{\partial x_3}$, is also given by the curvature, κ .

$$\frac{\partial \epsilon_{11}}{\partial x_3} = \frac{\partial^2 w}{\partial x_1^2} = \kappa \quad (3.3)$$

The displacement, w , was taken as the fundamental mode of the natural vibration of a cantilevered beam.

$$w = A[a(\sin(\beta_1 x) - \sinh(\beta_1 x)) + b(\cos(\beta_1 x) - \cosh(\beta_1 x))] \quad (3.4)$$

Where, $A = \frac{C_1}{a}$ and C_1 is the amplitude. $a = \sin(\beta_1 L) - \sinh(\beta_1 L)$, $b = \cos(\beta_1 L) + \cosh(\beta_1 L)$ and $\beta_1 L = 1.875$.

Normalizing the vertical displacement by A , $\bar{w} = \frac{w}{A}$ and using $\bar{x} = \frac{x}{L}$ equation (3.4) becomes

$$\bar{w} = a(\sin(\beta_1 L \bar{x}) - \sinh(\beta_1 L \bar{x})) + b(\cos(\beta_1 L \bar{x}) - \cosh(\beta_1 L \bar{x})) \quad (3.5)$$

After measuring the displacement, w , at $\bar{x} = 0.18$ and $\bar{x} = 0.67$, for increasing end loading (10 measurements at both locations), Cross et al. were able to determine the corresponding values of C_1 . With the values of C_1 in hand, the strain gradient values could be determined using equation (3.3). Doing so, they arrive at

$$\begin{aligned} \kappa &= \frac{\partial \epsilon_{11}}{\partial x_3} = \frac{\partial^2 w}{\partial x^2} \\ &= -A\beta_1^2 [a(\sin(\beta_1 x) + \sinh(\beta_1 x)) + b(\cos(\beta_1 x) + \cosh(\beta_1 x))] \end{aligned} \quad (3.6)$$

Using $\bar{\kappa} = \frac{\kappa L^2}{A(\beta_1 L)^2}$ to normalize the curvature (or strain gradient), they find

$$\bar{\kappa} = -[a(\sin(\beta_1 L \bar{x}) + \sinh(\beta_1 L \bar{x})) + b(\cos(\beta_1 L \bar{x}) + \cosh(\beta_1 L \bar{x}))] \quad (3.7)$$

Finally, the polarization values that were calculated using equation (3.1) were plotted against the corresponding strain gradient values found in equation (3.6). The slope of the linear line gave the flexoelectric coefficient value at the two locations. Figure 14 shows this plot.

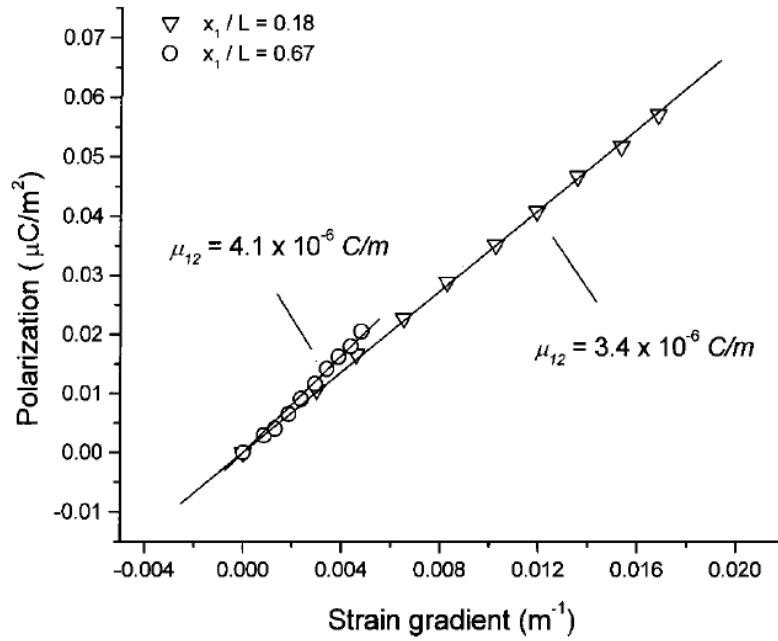


Figure 14: Cross et al. [10] result showing Polarization versus strain gradient for two locations on the beam

As figure 14 shows, at $\bar{x} = 0.18$, a flexoelectric coefficient value of $\mu_{12} = 3.4 \frac{\mu C}{m}$ was found and at $\bar{x} = 0.67$, $\mu_{12} = 4.1 \frac{\mu C}{m}$.

In an attempt to recreate the experimental setup used by Cross et al. and use the equations derived in chapter 2, we assume that a vertical force F (per length) is applied upwards to the end of a cantilevered bar of length L . Figure 15 illustrates our setup.

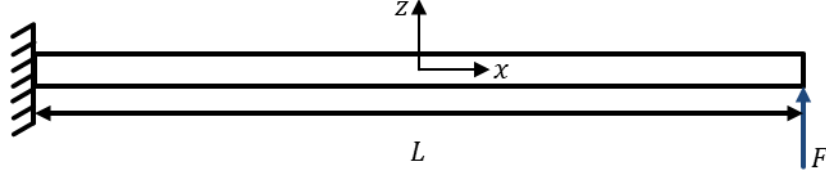


Figure 15: Schematic of the setup used to recreate the Cross et al. experiment

The moment (per length) in the bar is given by

$$M(x) = -Fx + FL \quad (3.8)$$

Using equations (2.29) and (2.30) and noting that $\kappa_2 = 0$, we find that equation (2.29) becomes

$$\Phi = \frac{L_3}{\epsilon} (D + \mu\kappa_1) \quad (3.9)$$

Similarly, equation (2.30) becomes

$$m_1 = \tilde{D}\kappa_1 + \frac{\mu L_3}{\epsilon} D \quad (3.10)$$

Solving for the electric displacement, D , from equation (3.9) and using it in equation (3.10), along with equation (3.8), we arrive at

$$\tilde{D}\kappa_1 + \frac{\mu L_3}{\epsilon} \left(\frac{\Phi \epsilon}{L_3} - \mu\kappa_1 \right) = -Fx + FL$$

Rearranging the terms, we have

$$\left(\tilde{D} - \frac{\mu^2 L_3}{\epsilon} \right) \kappa_1 = -\mu\Phi - Fx + FL$$

The term in parenthesis is \tilde{D}_{eff} as defined in equation (2.37). With $\kappa_1 = \frac{\partial^2 w_1}{\partial x^2}$, we have

$$\tilde{D}_{eff} \frac{\partial^2 w_1}{\partial x^2} = -\mu\Phi - Fx + FL$$

Since there is no applied voltage across the sample, we can assume that $\Phi = 0$, and we have that

$$\kappa_1 = \frac{\partial^2 w_1}{\partial x^2} = \frac{F}{\tilde{D}_{eff}} (-x + L) \quad (3.11)$$

Note that we have used κ_1 and w_1 to differentiate between the curvature and vertical displacement from Cross et al. Integrating twice and using the fact that $w_1 = 0$ at $x = 0$ and $\frac{\partial w_1}{\partial x} = 0$ at $x = 0$, we find

$$w_1 = \frac{F}{\tilde{D}_{eff}} \left(-\frac{1}{6}x^3 + \frac{L}{2}x^2 \right) \quad (3.12)$$

Next, with $\bar{x} = \frac{x}{L}$, $\bar{w}_1 = \frac{w_1 \tilde{D}_{eff}}{L^3 F}$ and $\bar{\kappa}_1 = \frac{\kappa_1 \tilde{D}_{eff}}{L F}$ we have

$$\bar{\kappa}_1 = -\bar{x} + 1 \quad (3.13)$$

$$\bar{w}_1 = -\frac{1}{6}\bar{x}^3 + \frac{1}{2}\bar{x}^2 \quad (3.14)$$

Equations (3.11) and (3.12) are corresponding equations to Cross et al. equations (3.6) and (3.4). C_1 in equation (3.4) corresponds to $\frac{F}{\tilde{D}_{eff}}$ in equation (3.12). Yet, it is important to note that equation (3.4) does not take into account the flexoelectric property of the sample and how that flexoelectric property may affect the vertical displacement. However, equation (3.12) does account for the flexoelectric property of the sample through the effective flexural rigidity, \tilde{D}_{eff} .

The values of polarization and strain gradient in [10] were presented as a plot (figure 15), not a table. Hence, the values of polarization and strain gradient were read from the plot by carefully passing vertical and horizontal lines through each data point. ($\bar{x} = 0.18, \bar{x} = 0.67$, 20 data points in all).

The objective is to construct a similar plot of polarization vs. strain gradient using equations (3.11) and (3.12). Because we have no way of determining the polarization, we will use the values read from figure 15. Yet, we are able to calculate strain gradient (curvature) values using equations (3.11) and (3.12), and using the strain gradient values read from figure 15. This is done by using (matching) the displacement values that can be calculated from the strain gradient values read in figure 15 to calculate the strain gradient using equations (3.11) and (3.12). The following are the steps taken to do so:

1. Determine the values of C_1 in equations (3.4) and (3.6):

Using equation (3.7), at $\bar{x} = 0.18$, $\bar{\kappa} = -4.57$ and at $\bar{x} = 0.67$, $\bar{\kappa} = -0.98$. Then,

$$\bar{\kappa} = \frac{\kappa L^2}{A(\beta_1 L)^2} = \frac{a\kappa L^2}{C_1(\beta_1 L)^2}$$

Thus, we have

$$C_1 = \frac{a\kappa L^2}{\bar{\kappa}(\beta_1 L)^2}$$

Using the values of the strain gradient determined from figure 15 for the strain gradient (κ), (10 values at $\bar{x} = 0.18$ and 10 values at $\bar{x} = 0.67$) we can determine the values of C_1 at each of the two locations.

2. Determine the values of the displacement w from equation (3.4) at each of the two locations using the values of C_1 :

Using equation (3.5), at $\bar{x} = 0.18$, $\bar{w} = -0.31$ and at $\bar{x} = 0.67$, $\bar{w} = -3.35$. Then,

$$\bar{w} = \frac{w}{A} = \frac{aw}{C_1}$$

Thus, we have

$$w = \frac{C_1}{a} \bar{w}$$

Using the values of C_1 that were determined in the previous step, we can determine the displacement at each of the two locations.

3. Determine the values of $\frac{F}{\bar{D}_{eff}}$ at each of the two locations using the values of w determined in the previous step:

Here, we “match” the displacement values that we found in the previous step, and use them as the displacement values in equation (3.12) to find $\frac{F}{\bar{D}_{eff}}$. Hence, $w = w_1$.

Using equation (3.14), at $\bar{x} = 0.18$, $\bar{w}_1 = 0.015$ and at $\bar{x} = 0.67$, $\bar{w}_1 = 0.174$. Then,

$$\bar{w}_1 = \frac{w_1 \bar{D}_{eff}}{L^3 F}$$

Thus, we have

$$\frac{F}{\tilde{D}_{eff}} = \frac{w_1}{L^3 \bar{w}_1}$$

Using the values of w from the previous step, we find the $\frac{F}{\tilde{D}_{eff}}$ values at each of the two locations.

4. Finally, determine the values of strain gradient (curvature) at each of the two locations using the values of $\frac{F}{\tilde{D}_{eff}}$ determined in the previous step:

Using equation (3.13), at $\bar{x} = 0.18$, $\bar{\kappa}_1 = 0.82$ and at $\bar{x} = 0.67$, $\bar{\kappa}_1 = 0.33$. Then,

$$\bar{\kappa}_1 = \frac{\kappa_1 \tilde{D}_{eff}}{LF}$$

Then, we have

$$\kappa_1 = \frac{F}{\tilde{D}_{eff}} \bar{\kappa}_1 L$$

Using the values of $\frac{F}{\tilde{D}_{eff}}$ from the previous step, we find the values of κ_1 at each of the two locations. Hence, we are able now to plot the polarization verses the strain gradient (curvature) determined using equations (3.11) and (3.12). Figure 16 is a recreation of figure 14 and is used to show that the values of polarization and strain gradient that were read from figure 14 are, in fact, accurately read. Figure 17 shows the polarization verses the strain gradient (curvature) calculated using equations (3.11) and (3.12).

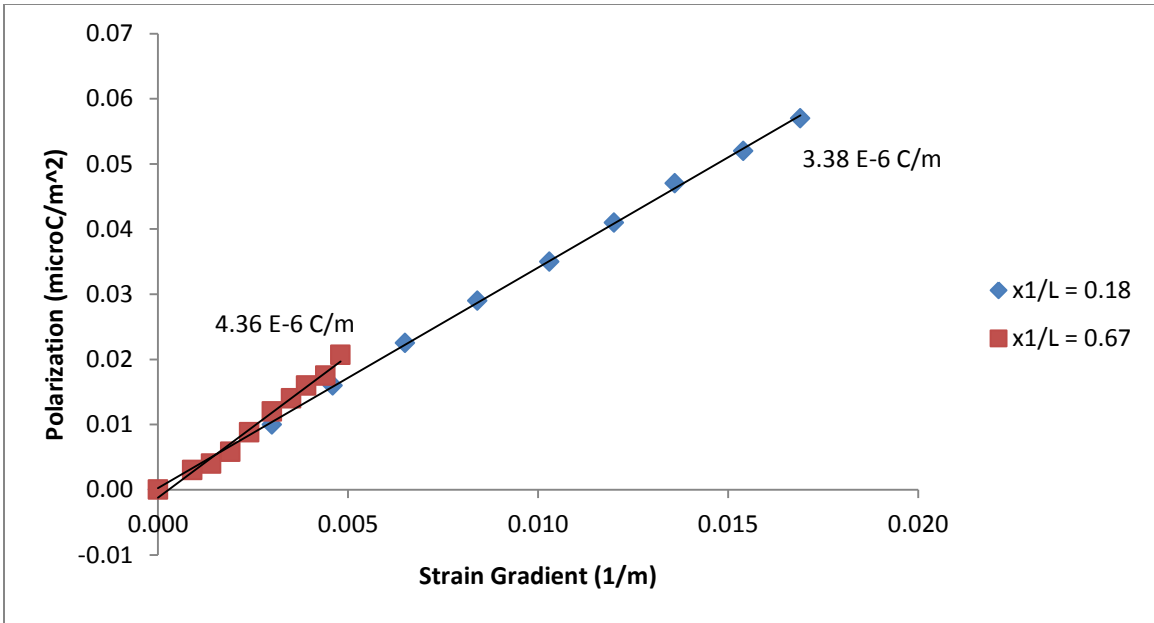


Figure 16: Plot recreating Polarization vs. Strain Gradient data from figure 15

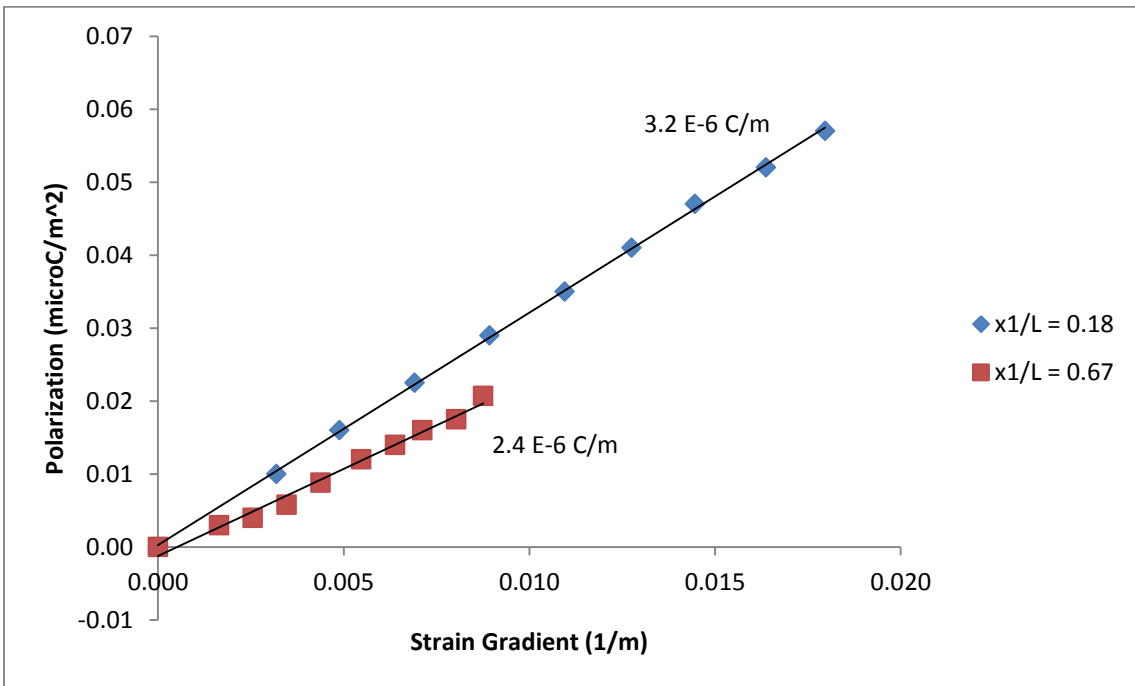


Figure 17: Plot of Polarization vs. Strain Gradient determined using equations (3.11) and (3.12)

As shown in figure 17, we find that at $\bar{x} = 0.18$, $\mu_{12} = 3.2 \frac{\mu C}{m}$ and $\bar{x} = 0.67$, $\mu_{12} = 2.4 \frac{\mu C}{m}$. While we were hoping to find flexoelectric coefficient values that were equal at the two locations, we are encouraged that the flexoelectric coefficient values we found are quite close to the experimental values.

Baskaran et al. (2012) [11] method for measuring flexoelectric coefficient:

Sample:

α -phase PVDF film with dimensions of Length (L) = 55mm, Width (h) = 20 mm, Thickness = $13.5 \mu m$.

Approach:

α -phase PVDF film, with grounding electrode fabricated on bottom surface of film, is glued to the top surface of cantilevered beam with high strength epoxy to form an effective beam system. Figure 18 shows the experimental setup.

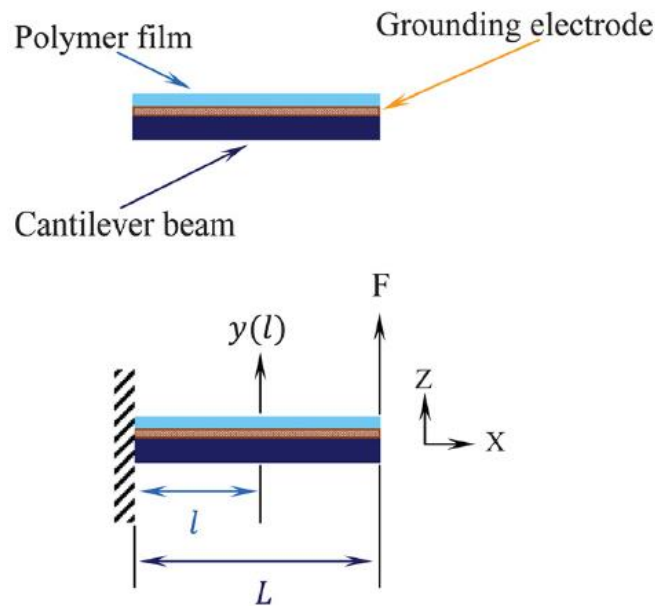


Figure 18: Schematic of experimental setup by Baskaran et al. in [11]

The sample is cantilevered at one end. At the opposite end, a dynamic loading tester (DLT) was used to displace the sample at a frequency of $f = 0.5 \text{ Hz}$. The location of the top electrode on the PVDF film was at $\bar{x} = \frac{x}{L} \approx 0.2$. Baskaran et al. use same approach as Cross et al. to determine the effective flexoelectric coefficient. That is they plot the polarization that they calculate using equation (3.1) against the strain gradient. However, the goal of the paper was to compare the value obtained for the effective flexoelectric coefficient of α -phase PVDF when using the Cross et al. displacement (equation 3.4)) to that obtained when using static deflection of the beam. This static deflection is almost identical to our equation (3.12).

The static deflection used by Baskaran et al. is given by

$$y = A_2 x^2 (3L - x) \quad (3.15)$$

Where $A_2 = -\frac{F}{6EI}$ and F is the end load. The negative sign comes from the fact that Baskaran et al. have taken the magnitude of the strain gradient to equal the curvature, while we've taken the strain gradient to equal the curvature. Rewriting equation (3.15) and multiplying by negative one, we have

$$y = \frac{F}{EI} \left(-\frac{1}{6} x^3 + \frac{L}{2} x^2 \right) \quad (3.16)$$

Comparing this equation to equation (3.12), we see that they are almost identical.

$$w_1 = \frac{F}{\tilde{D}_{eff}} \left(-\frac{1}{6} x^3 + \frac{L}{2} x^2 \right)$$

It is important to note that the coefficients in front of the two equations are different. \tilde{D}_{eff} is an effective flexural rigidity incorporating the effect of flexoelectricity, while EI represents the bending rigidity.

Baskaran et al. also presented the results of the comparison in a plot, and hence, the values of polarization and strain gradient were read from the plot. Figure 19 shows this plot.

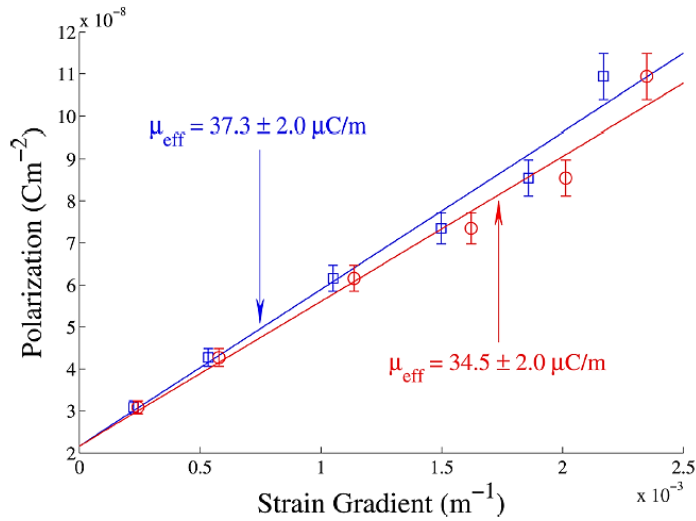


Figure 19: Polarization versus strain gradient from Baskaran et al. [11]. The blue line and points represent values obtained using Cross et al. equation (3.4) while the red line and points represent values obtained using equation (3.16)

By following the same steps used for reading polarization and strain gradient values from figure 14, we would expect to get identical values for strain gradient, as Baskaran et al. Hence, our plot of Polarization vs. Strain gradient using equation (3.12) would be the same as Baskaran et al. (red line and points on figure 19). However, we can use the values of strain gradient from the blue line and points in figure 19, which Baskaran et al. obtained using Cross et al. equation (3.4), to find a comparative value of the flexoelectric coefficient by using our equation (3.12). By following the same steps as before we can find our corresponding strain gradient values.

Figure 20 is a recreation of figure 19. As before, this recreation is used to show that the values of polarization and strain gradient that were read from figure 19 are, in fact, accurately read. Figure 21 shows our plot of Polarization versus strain gradient, with strain gradient obtained using equation (3.12).

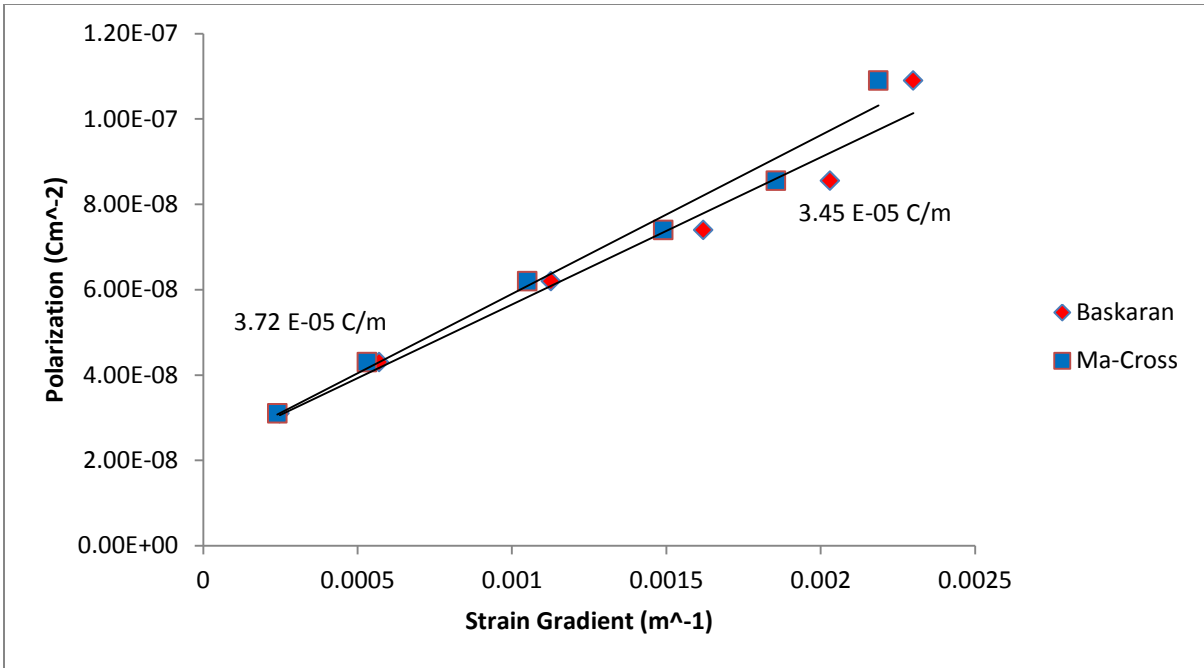


Figure 20: Plot recreating Polarization vs. Strain Gradient data from figure 20

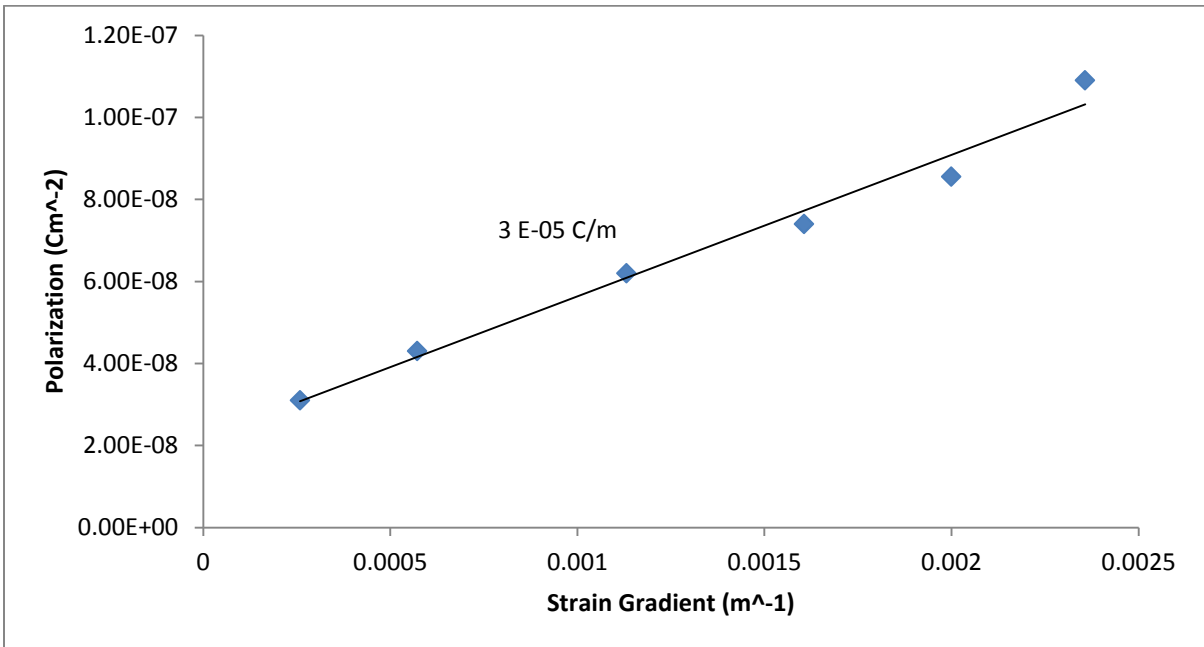


Figure 21: Polarization vs. Strain Gradient from [11] using equation (3.12)

While we expect to find identical results to Baskaran et al, our flexoelectric coefficient value is around $30 \frac{\mu C}{m}$, which is about $4 \frac{\mu C}{m}$ less than Baskaran et al. While the exact reason for this is unclear, we find that the displacement values obtained by using Cross et al. equation (3.4) are not the same as the displacement values obtained by using Baskaran et al. static loading, equation (3.16). This difference should not exist since Baskaran et al. took measurements of displacement and current, then modeled the deflection of the beam using two different models; Cross et al.'s equation (3.4), and the static deflection, equation (3.16). The table below shows this discrepancy.

Table 2: Comparison of displacement values obtained using equation (3.16) (Baskaran et al.) and equation (3.4) (Cross et al.)

Equation (3.16) (Baskaran et al.) Displacement (m)	Equation (3.4) (Cross et al.) Displacement (m)
1.92892E-08	2.012E-08
4.43342E-08	4.45155E-08
8.75794E-08	8.80249E-08
1.26002E-07	1.24912E-07
1.57892E-07	1.55511E-07
1.78892E-07	1.83343E-07

3.2 CONVERSE FLEXOELECTRIC EFFECT

To illustrate the use of equations (2.29 – 2.33), we consider a membrane that is subject to no external forces or moments. It is however subject to an applied voltage, Φ . We are interested in the effect of the applied voltage on the curvature of the membrane. The moment and force throughout the membrane is zero and the curvature and strain in

the 1 and 2 directions will be equal ($\kappa_1 = \kappa_2 = \kappa, \varepsilon_1 = \varepsilon_2 = \varepsilon$). Hence, equations (2.29) and (2.30) become

$$\Phi = \frac{L_3}{\varepsilon}(D + 2\mu\kappa) \quad (3.17)$$

$$m_1 = \tilde{D} \left[\frac{3}{2}\kappa \right] + \frac{\mu L_3}{\varepsilon} D = 0 \quad (3.18)$$

Solving for D from equation (3.18) and using the result it in equation (3.17), we find

$$\Phi = \frac{L_3}{\varepsilon} \left(-\frac{3}{2} \frac{\tilde{D}\varepsilon}{\mu L_3} \kappa + 2\mu\kappa \right)$$

Simplifying and solving for κ , we find

$$\kappa = \frac{\Phi}{\left(-\frac{3}{2} \frac{\tilde{D}}{\mu} + \frac{2\mu L_3}{\varepsilon} \right)} \quad (3.19)$$

We note that the curvature, κ , has a nonlinear relationship with the flexoelectric coefficient, μ . Re-arranging the terms in the denominator, we find that

$$\kappa = -\frac{2\mu\Phi}{3\tilde{D}} \left(\frac{1}{1 - \frac{4\mu^2 L_3}{3\tilde{D}\varepsilon}} \right)$$

Using $\tilde{D} = \frac{GL_3^3}{3}$ in the expression for κ , we can write

$$\kappa = -\frac{2\mu\Phi}{GL_3^3} \left(\frac{1}{1 - \left(\frac{L_c}{L_3} \right)^2} \right) \quad (3.20)$$

Here, L_c is a critical thickness of the membrane, like the one in equation (2.38), and is given by

$$L_c = \sqrt{\frac{4\mu^2}{\varepsilon G}} \quad (3.21)$$

Given ‘positive’ Φ , and material properties $G, \varepsilon, \mu > 0$, we see that for $L_3 > L_c$, we have $\kappa < 0$, which is consistent with other experimental observations [12]. If $L_3 <$

L_c , then the Helmholtz free energy of the membrane is not positive-definite, and the system becomes unstable. Note that in equation (3.21), the coefficient of 4 results from biaxial bending.

3.3 BENDING OF MEMBRANES

In this section, we consider situations where the membrane is subjected to a uniform electric field through the application of voltage, Φ , and tensile or compressive force loading, p . The force is applied in the x direction for the sake of illustration and, Figure 22 below shows the membrane under tensile force loading.

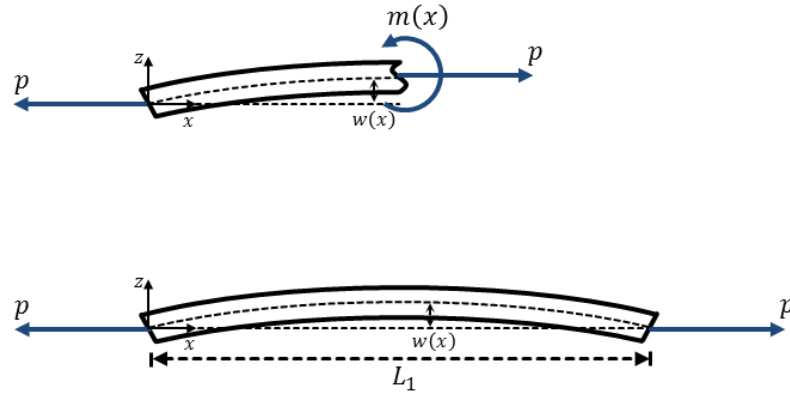


Figure 22: Schematic of membrane under in-plane loading

The effects of shear are neglected as the material under consideration is a soft elastomer. Based on a summation of moments on the left end of the membrane, we have that

$$m(x) = pw \quad (3.22)$$

Using equation (2.30) for the moment, we have

$$m_1 = m(x) = \tilde{D} \left[\kappa_1 + \frac{1}{2} \kappa_2 \right] + \frac{\mu L_3}{\epsilon} D = pw \quad (3.23)$$

Solving for D from equation (2.29), we find that

$$D = \frac{\epsilon \Phi}{L_3} - \mu \kappa$$

Next, we use the expression for D above in equation (3.23). Since $\kappa_2 = 0$ for this consideration, we have that

$$\tilde{D}\kappa_1 + \mu\Phi - \frac{\mu^2 L_3}{\epsilon}\kappa_1 = pw$$

Collecting similar terms, we arrive at

$$\left(\tilde{D} - \frac{\mu^2 L_3}{\epsilon}\right)\kappa_1 - pw = -\mu\Phi$$

The term in parenthesis is the effective flexural rigidity, \tilde{D}_{eff} , as defined in section 2.4.

Noting that $\kappa_1 = \frac{d^2w}{dx^2}$, we find

$$\frac{d^2w}{dx^2} + k^2w = -\frac{\mu\Phi}{\tilde{D}_{eff}} \quad (3.24)$$

Here, we have used that

$$\tilde{D}_{eff} = \tilde{D} - \frac{\mu^2 L_3}{\epsilon} \quad (3.25)$$

And

$$k^2 = -\frac{p}{\tilde{D}_{eff}} \quad (3.26)$$

The solution of the differential equation (3.24) is given by

$$w(x) = A\sin(kx) + B\cos(kx) + \frac{\mu\Phi}{p} \quad (3.27)$$

In order to better understand our results, we will consider three cases. In the first case, we assume that the membrane is not flexoelectric and that no voltage is applied. In the second case, we assume that the membrane is flexoelectric, but that no voltage is applied. Finally, in the third case, we assume that the membrane is flexoelectric and that voltage is applied. In all these cases, we assume that the membrane has no out-of-plane deflection at $x = 0$ and $x = L_1$. That is, $w(0) = 0$ and $w(L_1) = 0$.

Case 1: Membrane is not flexoelectric ($\mu = 0$) and no voltage is applied ($\Phi = 0$)

In this case, equation (3.25) reduces to $\tilde{D}_{eff} = \tilde{D}$ and equation (3.26) reduces to $k^2 = -\frac{p}{\tilde{D}}$ as $\mu = 0$. With $\tilde{D} > 0$ as a material property, we consider two situations:

i. Compression with $p < 0$ (Buckling)

In this situation, we would have $k^2 > 0$ and the solution from equation (3.27) becomes

$$w(x) = A\sin(kx) + B\cos(kx)$$

Using the boundary conditions, we find that $B = 0$ and $k = \frac{n\pi}{L_1}$ for $n \geq 1$. The critical p required for buckling would be

$$p_c = -\frac{\pi^2 \tilde{D}}{L_1^2} \quad (3.28)$$

This result is the expected result from a mechanics analysis.

ii. Tension with $p > 0$

In this situation, we would have $k^2 < 0$. Using the boundary conditions, we would find that $w = 0$. Hence, there is no out-of-plane displacement. This too is to be expected.

Case 2: Membrane is flexoelectric ($\mu \neq 0$) but no voltage is applied ($\Phi = 0$)

In this case, it is important to recognize that the sign of k^2 from equation (3.26) depends not only on the sign of p , but also on the sign of \tilde{D}_{eff} from equation (3.25). Examining equation (3.25), we note that it can be rewritten as

$$\tilde{D}_{eff} = \tilde{D} \left(1 - \frac{9\mu^2}{E\epsilon L_3^2} \right) = \tilde{D} \left(1 - \left(\frac{L_c}{L_3} \right)^2 \right)$$

Here, we have used the fact that $\tilde{D} = \frac{GL_3^3}{3}$ as we have done so in previous sections. L_c is the critical thickness that was defined in equation (2.38).

$$L_c = \sqrt{\frac{3\mu^2}{G\epsilon}}$$

Hence, for $L_3 > L_c$, $\tilde{D}_{eff} > 0$, and the sign of k^2 depends only on the sign of p . It follows that for $p < 0$ (buckling), the critical load required for buckling will be

$$p_c = -\frac{\pi^2 \tilde{D}_{eff}}{L_1^2} \quad (3.29)$$

For $p > 0$, we would still have no out-of-plane displacement, $w = 0$.

For $L_3 < L_c$, we would have $\tilde{D}_{eff} < 0$. As discussed in section 2.4, to ensure a positive-definite Helmholtz free energy, W , we must require that $\tilde{D}_{eff} > 0$, which implies that $L_3 > L_c$.

Case 3: Membrane is flexoelectric ($\mu \neq 0$) and voltage is applied ($\Phi \neq 0$)

In this case, it is important to first determine the out-of-plane displacement, w , of the membrane without the application of in-plane loading, p . That is, the out-of-plane displacement only due to the flexoelectric effect. When $p = 0$, equation (3.24) reduces to

$$\frac{d^2 w}{dx^2} = -\frac{\mu\Phi}{\tilde{D}_{eff}} \quad (3.30)$$

Integrating twice and using the boundary conditions, we arrive at

$$w(x) = \frac{\mu\Phi}{2\tilde{D}_{eff}} (L_1 x - x^2) \quad (3.31)$$

To understand the behavior of the membrane as the applied voltage is increased, we normalize equation (3.31) by the thickness, L_3 , and define $\bar{w} = \frac{w}{L_3}$, $\bar{x} = \frac{x}{L_3}$ and $\bar{L}_1 = \frac{L_1}{L_3}$.

Then, we find that

$$\bar{w}(\bar{x}) = \frac{\mu\Phi L_3}{2\tilde{D}_{eff}} (\bar{L}_1 \bar{x} - \bar{x}^2)$$

We note that $\frac{\tilde{D}_{eff}}{\mu L_3}$ is a voltage-like quantity, and use it to define the dimensionless voltage

$\bar{\Phi} = \frac{\Phi}{\frac{\tilde{D}_{eff}}{\mu L_3}}$. Doing so, we arrive at

$$\bar{w}(\bar{x}) = \frac{\bar{\Phi}}{2} (\bar{L}_1 \bar{x} - \bar{x}^2) \quad (3.32)$$

Figure 23 shows the behavior of the normalized membrane displacement in equation (3.32) for increasing values of $\bar{\Phi}$. In doing so, we assume the material properties of $BaTiO_3$ taken from [18]. The membrane thickness is taken to be $L_3 = 60 \text{ nm}$ and the membrane length is $L_1 = 50 * 60 \text{ nm} = 3 \mu\text{m}$. The effective flexural rigidity, \tilde{D}_{eff} , is well approximated by the flexural rigidity, \tilde{D} , as the critical thickness, $L_c \approx 0.28 \text{ nm}$. This critical thickness was obtained by using $\mu = 1 * 10^{-8} \frac{\text{C}}{\text{m}}$, $E = 130 \text{ GPa}$, and $\epsilon = 8.85 * 10^{-8} \frac{\text{C}^2}{\text{Nm}^2}$. Then we see that $\left(\frac{L_c}{L_3}\right)^2$ is of little significance. Hence, $\tilde{D}_{eff} \approx \tilde{D} = 3.12 * 10^{-12} \text{ J}$.

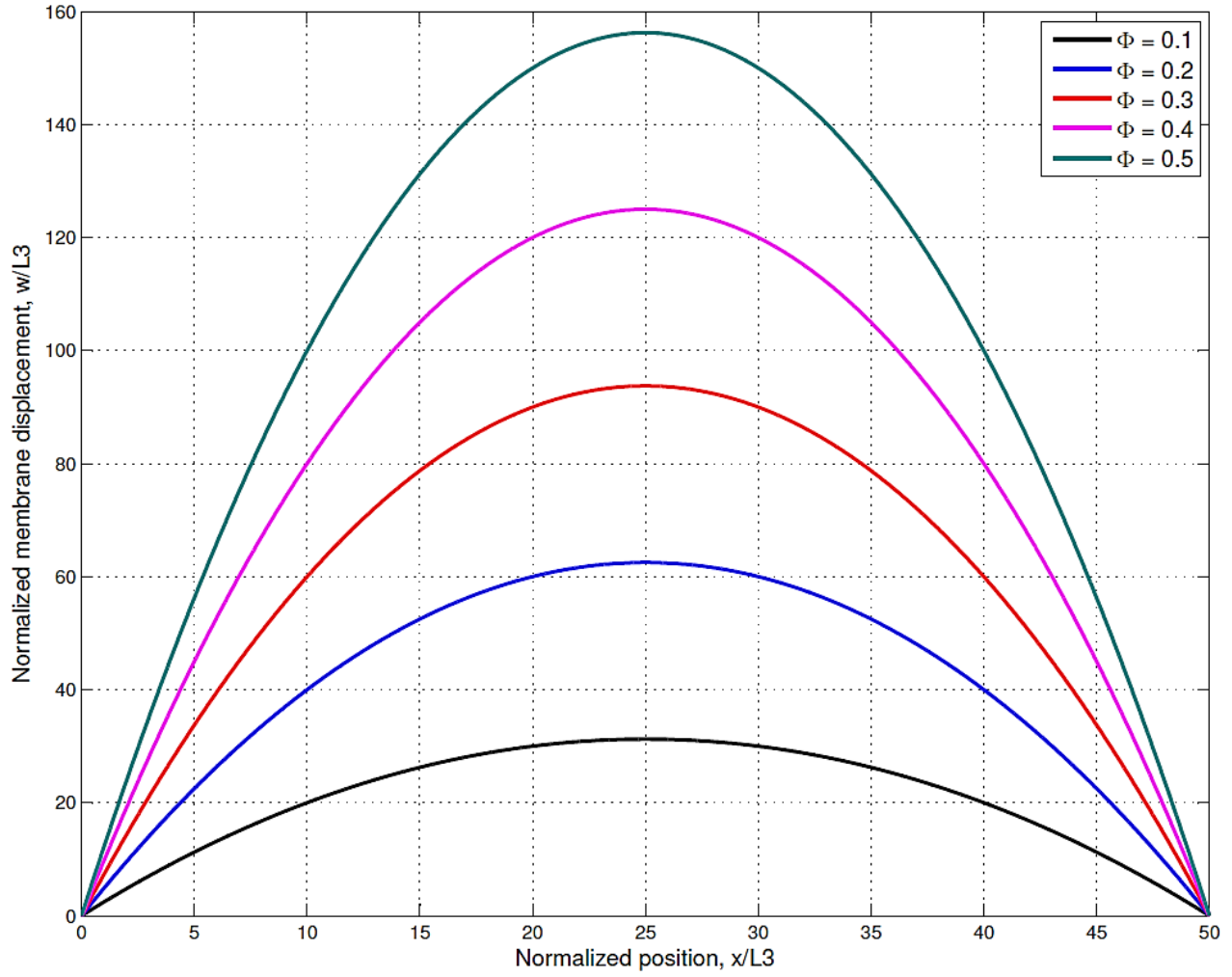


Figure 23: Normalized membrane displacement versus normalized position for increasing values of normalized applied voltage with no in-plane loading, $p = 0$

The maximum membrane displacement is achieved when $\bar{x} = \frac{\bar{L}_1}{2}$. Evaluating equation (3.32) at $\bar{x} = \frac{\bar{L}_1}{2}$, we arrive at

$$\bar{w}_{max}^{p=0} = \frac{\bar{\Phi} \bar{L}_1^2}{8} \quad (3.33)$$

From equation (3.33), we note that the maximum membrane displacement is linearly dependent on the normalized voltage.

Returning now to a condition where $p \neq 0$, and using the boundary condition that $w(0) = 0$, equation (3.27) becomes

$$w(x) = A \sin(kx) + \frac{\mu\Phi}{p} (1 - \cos(kx)) \quad (3.34)$$

Using the boundary condition that $w(L_1) = 0$, we find

$$A \sin(kL_1) + \frac{\mu\Phi}{p} (1 - \cos(kL_1)) = 0 \quad (3.35)$$

Next, using the trigonometric identity that $\sin(kL_1) = 2 \sin\left(\frac{kL_1}{2}\right) \cos\left(\frac{kL_1}{2}\right)$ and $1 - \cos(kL_1) = 2 \sin^2\left(\frac{kL_1}{2}\right)$, equation (3.35) simplifies to

$$\sin\left(\frac{kL_1}{2}\right) \left[A \cos\left(\frac{kL_1}{2}\right) + \frac{\mu\Phi}{p} \sin\left(\frac{kL_1}{2}\right) \right] = 0 \quad (3.36)$$

Equation (3.36) is satisfied when

$$\sin\left(\frac{kL_1}{2}\right) = 0 \quad (3.37)$$

Or when

$$A = -\frac{\mu\Phi}{p} \tan\left(\frac{kL_1}{2}\right) \quad (3.38)$$

From equation (3.37), and using equation (3.26) for k , the in-plane loading, p , is given by

$$p_n = -\frac{4n^2\pi^2}{L_1^2} \tilde{D}_{eff}$$

Using equation (3.38) in equation (3.34), we arrive at an expression for the membrane displacement given as

$$w(x) = \frac{\mu\Phi}{p} \left(1 - \cos(kx) - \tan\left(\frac{kL_1}{2}\right) \sin(kx) \right) \quad (3.39)$$

If $p \neq p_n$, then from equation (3.38), we recognize that $A \rightarrow \infty$ as $\frac{kL_1}{2} \rightarrow \frac{\pi}{2}$. Therefore, $k \rightarrow \frac{\pi}{L_1}$. Using equation (3.26) again, we arrive at

$$p_c = -\frac{\pi^2}{L_1^2} \tilde{D}_{eff} \quad (3.40)$$

This critical value of the in-plane loading is reached first as the membrane is gradually compressed.

To better observe the behavior of the membrane displacement in equation (3.39), we normalize it by L_3 as was previously done to equation (3.31). Hence, as before, we have $\bar{w} = \frac{w}{L_3}$, $\bar{x} = \frac{x}{L_3}$, $\bar{L}_1 = \frac{L_1}{L_3}$ and $\bar{\Phi} = \frac{\Phi}{\frac{D_{eff}}{\mu L_3}}$. Additionally, we define $\bar{k} = kL_3$. Doing so,

we arrive at

$$\bar{w}(\bar{x}) = -\frac{\bar{\Phi}}{\bar{k}^2} \left(1 - \cos(\bar{k}\bar{x}) - \tan\left(\frac{\bar{k}\bar{L}_1}{2}\right) \sin(\bar{k}\bar{x}) \right) \quad (3.41)$$

Figure 24 shows the behavior of the normalized out-of-plane displacement in equation (3.41) as the membrane is gradually compressed by in-plane loading, p . The in-plane loading is normalized by the magnitude of the critical in-plane loading, $|p_c|$. That is $\bar{p} = \frac{p}{|p_c|}$. The figure shows this behavior for a given applied voltage which we've taken to be $\bar{\Phi} = 0.1$.

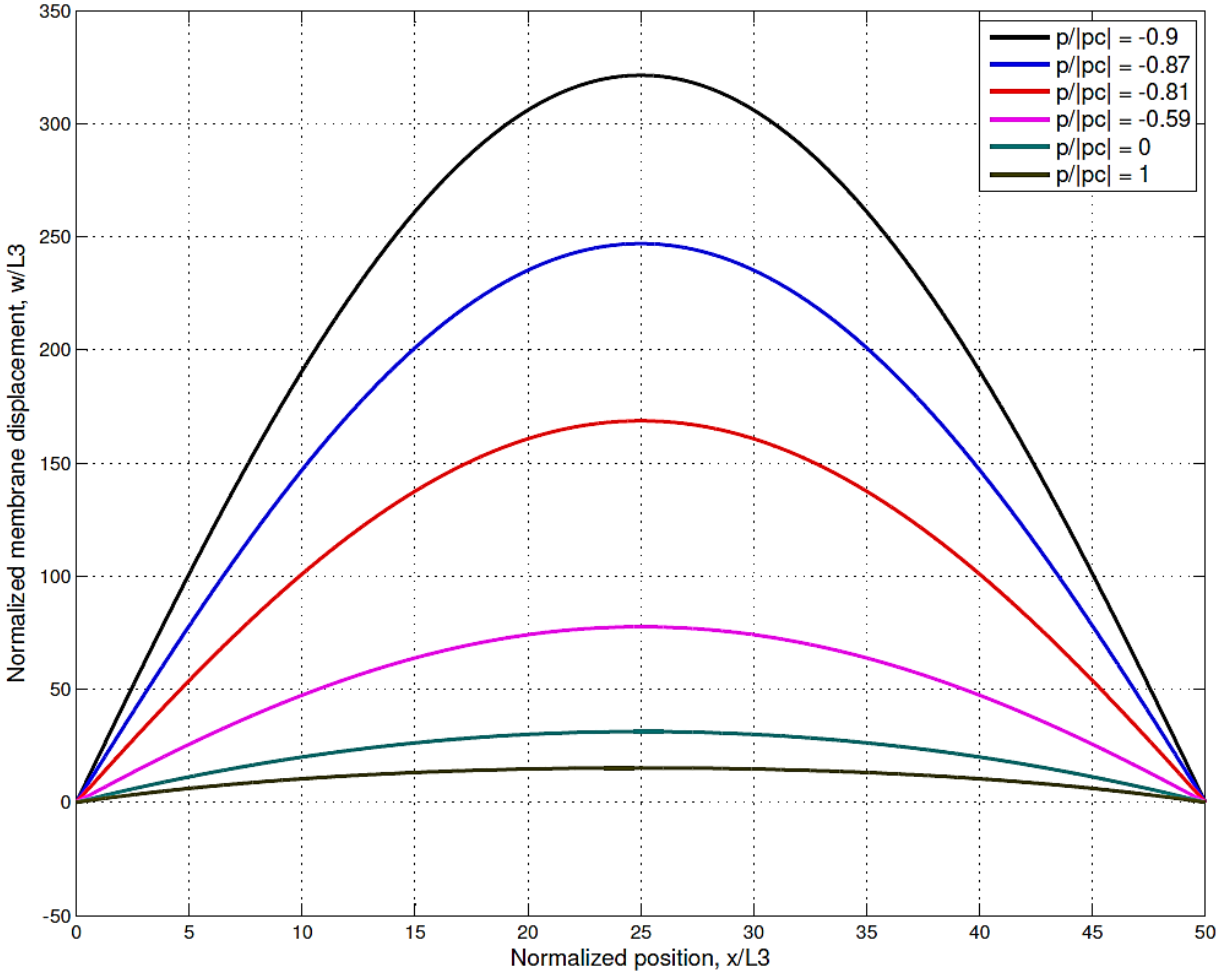


Figure 24: Normalized membrane displacement versus normalized position for increasingly compressive values of in-plane loading with $\bar{\Phi} = 0.1$

We see that as the in-plane loading approaches to the critical value in equation (3.40), the membrane displacement increases rapidly. This behavior is better illustrated by plotting the maximum membrane displacement as a function of in-plane loading. The normalized maximum membrane displacement occurs at $\bar{x} = \frac{1}{2}$, and hence we have

$$\bar{w}_{max} = -\frac{\bar{\Phi}}{\bar{k}^2} \left(1 - \cos\left(\frac{\bar{k}L_1}{2}\right) - \tan\left(\frac{\bar{k}L_1}{2}\right) \sin\left(\frac{\bar{k}L_1}{2}\right) \right) \quad (3.42)$$

Figure 25 shows the normalized maximum membrane displacement as a function of normalized in-plane loading, \bar{p} , for increasing values of the normalized applied voltage,

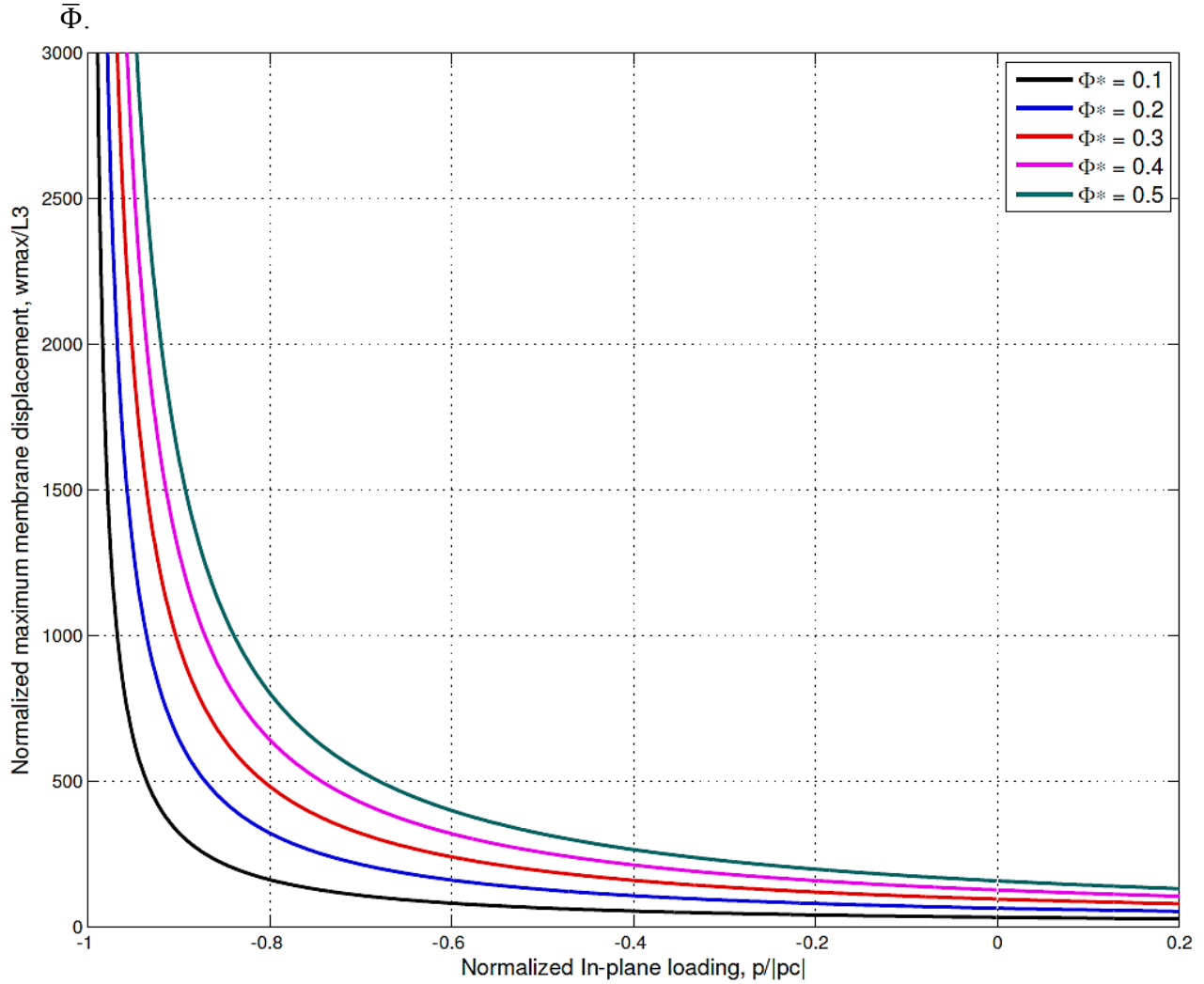


Figure 25: Normalized maximum membrane displacement versus normalized in-plane loading for increasing values of normalized applied voltage

Figure 25 illustrates that as the in-plane loading becomes more compressive and reaches p_c , the maximum membrane displacement blows up and goes to infinity. When the in-plane loading is tensile, the membrane displacement approaches zero asymptotically. Additionally, as the applied voltage is increased, the membrane

displacement is aided by the applied voltage and increases even faster as the membrane is compressed.

3.4 A MEMBRANE-SPRING MODEL

We return now to the cell membrane from Chapter 1 considered by Brownell et al. Brownell et al. [6] modeled the local stretching and contracting of outer hair cells by proposing that this stretching and contracting (called electromotility) was caused by the curvature changes in the membrane which are induced by the flexoelectric nature of the cell membrane. Brownell et al. modeled the cell membrane as a curved dielectric and flexoelectric surface connected at either end with a series of springs. The springs model the spectrin molecules which are embedded in the cortical lattice. Part of figure 7 in section 1.4, shown again below, illustrates this model.

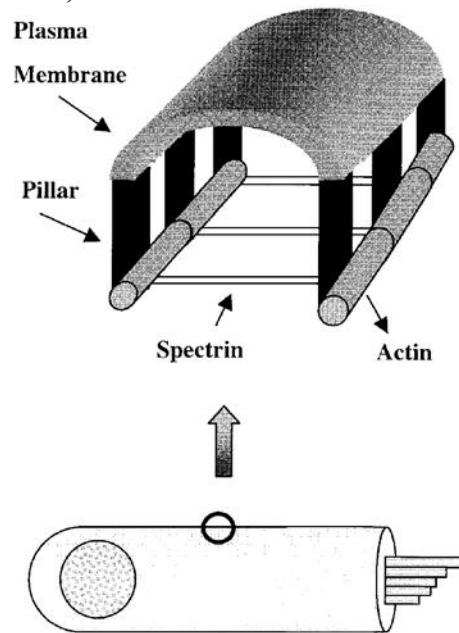


Figure 26: Illustration of a part of the cell (plasma) membrane of an outer hair cell [6]. The spectrin molecules are assumed to be connected to the plasma membrane by stiff pillars

Figure 27 shows a schematic of a membrane-spring model that we have considered, similar to Brownell et al. The linear springs model the spectrin molecules, which are connected to the ends of the membrane. We introduce a mismatch δ_0 between the membrane and the spring such that the initial length of the membrane is L_1 and the initial length of the spring is $L_1 - \delta_0$.

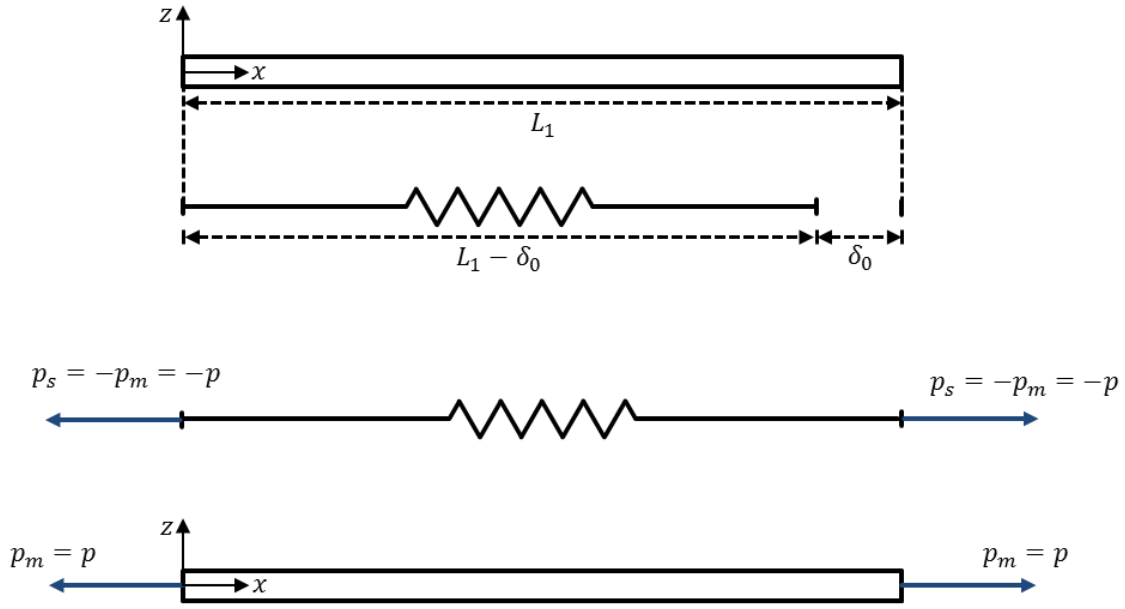


Figure 27: Schematic of a membrane-spring model, similar to Brownell et al.

The in-plane load acting on the membrane is p_m and the load from the springs is p_s . Since the ends of the membrane and springs are attached, their total length will be equal. Hence, once they are attached, we have

$$\begin{aligned} \Delta u_m + L_1 &= \Delta u_s + L_1 - \delta_0 \\ \Delta u_s &= \Delta u_m + \delta_0 \end{aligned} \quad (3.43)$$

In equation (3.43), Δu_m is the net change of length of the membrane in the x -direction, and Δu_s is the net change of length of the springs.

The in-plane loading on the membrane is related to the loading caused by the springs attached to the ends of the membrane. \mathcal{P}_s is defined as the total force due to the springs which are attached along the y -direction. The length of the membrane in this direction is L_2 . Hence, we have

$$\mathcal{P}_s = k_s \Delta u_s N \quad (3.44)$$

In equation (3.44), N is the number of linear springs along L_2 and k_s is the stiffness of each spring with dimensions of $\frac{Force}{Length}$. We then have that

$$p_s = \frac{\mathcal{P}_s}{L_2} = k_s \Delta u_s \frac{N}{L_2} = k_s \Delta u_s \frac{1}{s} = k_s \Delta u_s n$$

Here, s is the spacing between linear springs. Alternatively, n is the number of springs per length along L_2 . Thus, we have that

$$p_s = nk_s \Delta u_s \quad (3.45)$$

Noting that $p_s = -p_m = -p$, we use equation (3.43) in equation (3.45) and find

$$-p = nk_s (\Delta u_m + \delta_0) \quad (3.46)$$

To utilize the equation (3.46), we will first need to determine Δu_m . Using the results obtained for the out-of-plane displacement from the previous section for a flexoelectric membrane under in-plane loading and applied voltage, along with kinematic equations and the derived constitutive equations from chapter 2, we can find $u(x)$, the corresponding in-plane displacement of the membrane in the x -direction.

We begin as always with the constitutive equations. We assume, as before, that $\kappa_2 = 0$, and that there is no strain in the y -direction. Hence, $\varepsilon_2 = 0$. Using equation (2.29) and solving for the electric displacement, then using the electric displacement in equation (2.32) we find

$$p = 4L_3 G \varepsilon_1 - \frac{L_3}{\varepsilon} \left(\frac{\varepsilon \Phi}{L_3} - \mu \kappa_1 \right)^2 - \frac{2\mu L_3}{\varepsilon} \left(\frac{\varepsilon \Phi}{L_3} - \mu \kappa_1 \right) \kappa_1$$

After expansion and simplification, we arrive at

$$p = 4L_3G\varepsilon_1 - \frac{\epsilon\Phi^2}{L_3} + \frac{L_3}{\epsilon}(\mu\kappa_1)^2 \quad (3.47)$$

Next, from equation (3.39) for the out-of-plane displacement in case 3 of section 3.3, we had that

$$w(x) = \frac{\mu\Phi}{p}(1 - \cos(kx) - C \sin(kx))$$

Here, we've used that $C = \tan\left(\frac{kL_1}{2}\right)$ for convenience. From equation (3.25) and (3.26), we also had that $\tilde{D}_{eff} = \tilde{D} - \frac{\mu^2L_3}{\epsilon}$ and $k^2 = -\frac{p}{\tilde{D}_{eff}}$. We then use the kinematic relationship that we've used before that $\kappa_1 = \frac{\partial^2 w}{\partial x^2}$. Doing so, we find

$$\kappa_1 = \frac{\partial^2 w}{\partial x^2} = \frac{\mu\Phi k^2}{p}(\cos(kx) + C \sin(kx)) \quad (3.48)$$

Using equation (3.48) in equation (3.47), we solve for the strain in the x -direction, ε_1 . Doing so, we find

$$\begin{aligned} \varepsilon_1 = & \frac{\epsilon\Phi^2}{4L_3^2G} + \frac{p}{4L_3G} \\ & - \frac{\mu^2}{4G\epsilon} \left(\left(\frac{\mu\Phi}{p} \right)^2 k^4 (\cos^2(kx) + 2C \sin(kx) \cos(kx) \right. \\ & \left. + C^2 \sin^2(kx)) \right) \end{aligned} \quad (3.49)$$

It's useful to note that all the terms in equation (3.49) are dimensionless. Next, we use the kinematic equation given by

$$\frac{\partial u}{\partial x} = \varepsilon_1 - \frac{1}{2} \left(\frac{\partial w}{\partial x} \right)^2 \quad (3.50)$$

We will use the strain, ε_1 , from equation (3.49) and out-of-plane displacement, w , from equation (3.39) in equation (3.50) to solve for the derivative of the in-plane displacement $\frac{\partial u}{\partial x}$. Doing so, we get

$$\frac{\partial u}{\partial x} = \varepsilon_1 - \frac{1}{2} \left(\left(\frac{\mu\Phi}{p} \right)^2 k^2 (\sin^2(kx) - 2C \sin(kx) \cos(kx) + C^2 \cos^2(kx)) \right) \quad (3.51)$$

Integrating equation (3.51) with respect to x , we are able to find the in-plane displacement $u(x)$. After expansion and simplification, we find

$$\begin{aligned} u(x) = & \left[\frac{\epsilon\Phi^2}{4L_3^2G} + \frac{p}{4L_3G} - \left(\frac{\mu^4\Phi^2k^4}{8G\epsilon p^2} + \frac{\mu^2\Phi^2k^2}{4p^2} \right) (C^2 + 1) \right] x \\ & + \left[\frac{\mu^4\Phi^2k^3}{16G\epsilon p^2} - \frac{\mu^2\Phi^2k}{8p^2} \right] (C^2 - 1) \sin(2kx) \\ & - \left[\frac{\mu^4\Phi^2k^3}{8G\epsilon p^2} - \frac{\mu^2\Phi^2k}{4p^2} \right] C \cos(2kx) + c_1 \end{aligned}$$

To determine the integration constant, c_1 , we assume that there is no in-plane displacement at the left end of the membrane. That is, $u(x = 0) = 0$. Doing so, we find the integration constant to be

$$c_1 = \left[\frac{\mu^4\Phi^2k^3}{8G\epsilon p^2} - \frac{\mu^2\Phi^2k}{4p^2} \right] C$$

Finally, after more simplification, we arrive at

$$\begin{aligned} u(x) = & \left[\frac{\epsilon\Phi^2}{4L_3^2G} + \frac{p}{4L_3G} - \left(\frac{\mu\Phi}{p} \right)^2 \left(\frac{\mu^2k^4}{8G\epsilon} + \frac{k^2}{4} \right) (C^2 + 1) \right] x \\ & + \left(\frac{\mu\Phi}{p} \right)^2 \left\{ \left[\frac{\mu^2k^3}{16G\epsilon} - \frac{k}{8} \right] (C^2 - 1) \sin(2kx) \right. \\ & \left. + \left[\frac{\mu^2k^3}{8G\epsilon} - \frac{k}{4} \right] C(1 - \cos(2kx)) \right\} \end{aligned} \quad (3.52)$$

Then, $\Delta u_m = u(x = L_1) - u(x = 0) = u(x = L_1)$. Hence, we find

$$\begin{aligned} \Delta u_m = & \left[\frac{\epsilon\Phi^2}{4L_3^2G} + \frac{p}{4L_3G} - \left(\frac{\mu\Phi}{p} \right)^2 \left(\frac{\mu^2k^4}{8G\epsilon} + \frac{k^2}{4} \right) (C^2 + 1) \right] L_1 \\ & + \left(\frac{\mu\Phi}{p} \right)^2 \left\{ \left[\frac{\mu^2k^3}{16G\epsilon} - \frac{k}{8} \right] (C^2 - 1) \sin(2kL_1) \right. \\ & \left. + \left[\frac{\mu^2k^3}{8G\epsilon} - \frac{k}{4} \right] C(1 - \cos(2kL_1)) \right\} \end{aligned} \quad (3.53)$$

Equation (3.53) represents the net in-plane displacement of the membrane in the x -direction due to in-plane loading and the application of voltage.

An illustrative, simple, problem would be a flexoelectric membrane without the application of voltage, as discussed in case 2 from section 3.3. In this case, equation (3.53) reduces to

$$\Delta u_m = \frac{pL_1}{4L_3G} \quad (3.54)$$

Using equation (3.54) in equation (3.46), and solving for the in-plane loading, we find

$$p = -\frac{\delta_0}{\left(\frac{1}{nk_s} + \frac{L_1}{4L_3G}\right)} \quad (3.55)$$

Equation (3.55) represents the in-plane loading caused by a mismatch, δ_0 . As expected, this in-plane loading depends on the material properties of the spring (nk_s) as well as the membrane (G). The critical in-plane loading required for buckling is given by equation (3.29) as follows

$$p_c = -\frac{\pi^2 \tilde{D}_{eff}}{L_1^2}$$

Using this in equation (3.55), we find that, for a flexoelectric membrane without the application of voltage, the critical mismatch required for a flexoelectric membrane to buckle is given by

$$\delta_{0c} = \left(\frac{1}{nk_s} + \frac{L_1}{4L_3G}\right) \frac{\pi^2 \tilde{D}_{eff}}{L_1^2} \quad (3.56)$$

If the membrane is under an applied voltage, then the problem becomes much more complex. This complexity arises from the fact that Δu_m in equation (3.53) depends on the in-plane loading, p , and the in-plane loading in equation (3.46) depends on Δu_m . If we are interested in the behavior of the in-plane loading as a function of applied voltage and initial mismatch, then we can solve for Δu_m from equation (3.46) and equate the result to equation (3.53), which gives

$$\begin{aligned}
-\frac{p}{nk_s} - \delta_0 = & \left[\frac{\epsilon\Phi^2}{4L_3^2G} + \frac{p}{4L_3G} - \left(\frac{\mu\Phi}{p}\right)^2 \left(\frac{\mu^2k^4}{8G\epsilon} + \frac{k^2}{4}\right) (C^2 + 1) \right] L_1 \\
& + \left(\frac{\mu\Phi}{p}\right)^2 \left\{ \left[\frac{\mu^2k^3}{16G\epsilon} - \frac{k}{8}\right] (C^2 - 1) \sin(2kL_1) \right. \\
& \left. + \left[\frac{\mu^2k^3}{8G\epsilon} - \frac{k}{4}\right] C(1 - \cos(2kL_1)) \right\}
\end{aligned} \tag{3.57}$$

Solving for p in equation (3.57) as a function of Φ and δ_0 for known material properties (G, ϵ, μ) might not seem too difficult until one recalls that $k^2 = -\frac{p}{\bar{D}_{eff}}$ and $C = \tan\left(\frac{kL_1}{2}\right)$.

An iterative solver could perhaps be used, but that undertaking is not done here.

Alternatively, if we are interested in the behavior of the net in-plane membrane displacement as a function of applied voltage and initial mismatch, then we can use equation (3.46) for p in equation (3.53) to find

$$\begin{aligned}
\Delta u_m = & \left[\frac{\epsilon\Phi^2}{4L_3^2G} - \frac{(nk_s(\Delta u_m + \delta_0))}{4L_3G} \right. \\
& - \left. \left(\frac{\mu\Phi}{nk_s(\Delta u_m + \delta_0)}\right)^2 \left(\frac{\mu^2k^4}{8G\epsilon} + \frac{k^2}{4}\right) (C^2 + 1) \right] L_1 \\
& + \left(\frac{\mu\Phi}{nk_s(\Delta u_m + \delta_0)}\right)^2 \left\{ \left[\frac{\mu^2k^3}{16G\epsilon} - \frac{k}{8}\right] (C^2 - 1) \sin(2kL_1) \right. \\
& \left. + \left[\frac{\mu^2k^3}{8G\epsilon} - \frac{k}{4}\right] C(1 - \cos(2kL_1)) \right\}
\end{aligned} \tag{3.58}$$

Solving for Δu_m as a function of Φ and δ_0 would be as challenging as solving for p in equation (3.58), and that undertaking is not done here. While equation (3.57) and (3.58) are difficult to solve, they demonstrate the complexities that arise in flexoelectric membranes.

Chapter 4: Conclusions

In a quest to better understand the effect of flexoelectricity in thin membrane, we have developed a set of constitutive equations (2.29) – (2.33) which relate the applied physical quantities to the state variables in a flexoelectric membrane.

By inspection of the Helmholtz free energy function of the membrane, we find a critical thickness, L_c , dependent on membrane's elastic, dielectric and flexoelectric constants. For membranes whose thickness is less than the critical thickness, the Helmholtz free energy function is no longer positive-definite.

We propose that one way to resolve the issue of a non-positive definite Helmholtz free energy is by sandwiching the membrane between two elastic electrodes. In doing so, we arrive at a critical thickness for the sandwiching layers, t_c , dependent on the elastic constant of the sandwiching layers, and on the dielectric and flexoelectric constants of the membrane being sandwiched.

Another way may be to account for more physical phenomena within the Helmholtz free energy. One example would be the inclusion of surface effects. Yet another way, as done by [18] – [20] is to include more coupling terms within the Helmholtz free energy. Coupling between polarization and polarization gradient, strain and polarization gradient and other higher order coupling was not included in our model. Future work may account for more physical phenomena and more coupling terms.

We have used our constitutive equations to replicate experimental attempts at calculating the flexoelectric coefficients of certain ceramics. In doing so, we have used the experimental data that was available on the experimental research papers. Our numerical results for the flexoelectric coefficients are very close to those published in the experimental research papers, giving us confidence in the validity of our model.

However, there is disagreement among researchers regarding the flexoelectric coefficients for soft materials [12], [21] – [23].

In studying the behavior of a flexoelectric membrane under the application of voltage and in-plane loading, we find that the critical load necessary for “buckling” depends on the flexoelectric coefficient as well as the dielectric permittivity of the membrane. However, the membrane is not buckling in the true sense, as there is out-of-plane displacement of the membrane caused by the application of voltage without any in-plane loading. As the in-plane loading is increasingly compressive and approaches the critical value, the maximum membrane displacement approaches infinity. If the membrane is in tension, the maximum membrane displacement approaches zero asymptotically. The application of voltage essentially aids the out-of-plane membrane displacement, and allows the membrane to “buckle” without the application of in-plane loading. This analysis is a linearized analysis and does not capture the exact behavior of the membrane for finite deformation.

Using a membrane-spring model similar to one proposed by Brownell et al., we investigated the behavior of the net in-plane displacement of a flexoelectric membrane which is attached at both ends to a series of springs and is under the application of voltage. Using the constitutive relations which were derived in chapter 2, along with the out-of-plane displacement found in section 3.3, we found the net in-plane displacement of the membrane. This result, however, is not easily solved as a function of applied voltage and initial mismatch, illustrating the complexities that arise in flexoelectric membranes.

References

- [1] Nguyen, T.D., Mao, S., Yeh, Y.W., Purohit, P.K., McAlpine, M.C., 2013, Nanoscale Flexoelectricity. *Adv. Mater.*, 25: 946–974
- [2] Jona, F., Shirane G., 1962, *Ferroelectric Crystals*. Pergamon Press Inc., New York
- [3] Meyer, R.B., 1969, Piezoelectric effects in liquid crystals. *Phys. Rev. Lett.* 22: 918–921
- [4] Winsor, P.A., 1968, Binary and multicomponent solutions of amphiphilic compounds. Solubilization and the formation, structure, and theoretical significance of liquid crystalline solutions. *Chem. Rev.* 68: 1-40
- [5] Tagantsev, A.K., 1987, Pyroelectric, piezoelectric, flexoelectric, and thermal polarization effects in ionic crystals. *Sov. Phys. Usp.* 30: 588–603
- [6] Raphael, R.M., Popel, A.S., Brownell, W.E., 2000, A membrane bending model of outer hair cell electromotility. *Biophys J.* 78: 2844-2862
- [7] Huang, R., Suo, Z., 2012, Electromechanical phase transition in dielectric elastomers. *Proc. R. Soc. A* 468: 1014-1040
- [8] Gent, A.N., 1996, A new constitutive relation for rubber. *Rubber Chem. Technol.* 69: 59–61
- [9] Timoshenko, S., Woinowsky-Krieger, S., 1959, *Theory of plates and shells* (2nd ed). McGraw-Hill, New York
- [10] Ma, W., Cross, L.E., 2001, Observation of the flexoelectric effect in relaxor $Pb\left(Mg_{\frac{1}{3}}Nb_{\frac{2}{3}}\right)O_3$ ceramics. *Appl. Phys. Lett.* 78: 2920–2921
- [11] Baskaran, S., He, X., Yang, Y., Fu, J.Y., 2012, Strain gradient induced electric polarization in alpha-phase polyvinylidene fluoride films. *Journal of Applied Physics.* 111: 014109
- [12] Zubko, P., Catalan, G., Tagantsev, A.K., 2013, Flexoelectric effect in Solids. *Annu. Rev. Mater. Res.* 43: 387–421
- [13] Ma, W., Cross, L.E., 2001, Large flexoelectric polarization in ceramic lead magnesium niobate. *Appl. Phys. Lett.* 79: 4420–4422
- [14] Ma, W., Cross, L.E., 2002, Flexoelectric polarization of barium strontium titanate in the paraelectric state. *Appl. Phys. Lett.* 81: 3440–3442
- [15] Ma, W., Cross, L.E., 2005, Flexoelectric effect in ceramic lead zirconate titanate. *Appl. Phys. Lett.* 86: 072905
- [16] Ma, W., Cross, L.E., 2006, Flexoelectricity of barium titanate. *Appl. Phys. Lett.* 88: 232902

- [17] Ma, W., Cross, L.E., 2003, Strain-gradient-induced electric polarization in lead zirconate titanate ceramics. *Appl. Phys. Lett.* 82: 3293–3295
- [18] Zhang, Z., Jiang, L.Y., 2014, Size effects on electromechanical coupling fields of a bending piezoelectric nanoplate due to surface effects and flexoelectricity. *Journal of Applied Physics*, 116: 134308
- [19] Yan, Z., Jiang, L.Y., 2013, Flexoelectric effect on the electroelastic responses of bending piezoelectric nanobeams. *Journal of Applied Physics*, 113: 194102
- [20] Tagantsev, A.K., Yurkov, A.S., 2012, Flexoelectric effect in finite samples. *Journal of Applied Physics*, 112: 044103
- [21] Eliseev, E.A., Morozovska, A.N., Glinchuk, M.D., Blinc, R., 2009, Spontaneous flexoelectric/flexomagnetic effect in nanoferroics. *Phys. Rev. B* 79: 165433
- [22] Ponomareva, I., Tagantsev, A.K., Bellaiche, L., 2012, Finite-temperature flexoelectricity in ferroelectric thin films from first principles. *Phys. Rev. B* 85: 104101
- [23] Gao, Y.F., Wang, Z.L., 2007, Electrostatic Potential in a Bent Piezoelectric Nanowire. *The Fundamental Theory of Nanogenerator and Nanopiezotronics. Nano Lett.* 7: 2499
- [24] Sachs, F., Brownell, W.E., Petrov, A.G., 2009, Membrane Electromechanics in Biology, with a focus on hearing. *MRS Bulletin*, 34: 665-670

Vita

Nebiyu Sermollo was born in Addis Ababa, Ethiopia. After completing his high school studies at Saint Joseph School, Addis Ababa, in 2008, he moved to Houston, TX, where he was admitted to the University of Houston. In 2012, he graduated with a Bachelor of Science degree in Mechanical Engineering and moved to Austin, TX, where he was accepted to the Graduate School at The University of Texas at Austin.

Email address: nebiyu.sermollo@utexas.edu

This thesis was typed by Nebiyu Barsula Sermollo.